Kaunas University of Technology

Faculty of Mathematics and Natural Sciences

Development of a Modular Radiometric Measurement System for Radiation Protection

Master's Final Degree Project

Andrejus Litvakas

Project author

Assoc. prof. dr. Benas Gabrielis Urbonavičius

Supervisor

Kaunas, 2023

Kaunas University of Technology

Faculty of Mathematics and Natural Sciences

Development of a Modular Radiometric Measurement System for Radiation Protection

Master's Final Degree Project

Medical Physics (6213GX001)

Andrejus Litvakas

Project author

Assoc. prof. dr. Benas Gabrielis Urbonavičius

Supervisor

Assoc. prof. dr. Vytautas Stankus

Reviewer

Kaunas, 2023

Kaunas University of Technology

Faculty of Mathematics and Natural Sciences

Andrejus Litvakas

Development of a Modular Radiometric Measurement System for Radiation Protection

Declaration of Academic Integrity

I confirm the following:

1. I have prepared the final degree project independently and honestly without any violations of the copyrights or other rights of others, following the provisions of the Law on Copyrights and Related Rights of the Republic of Lithuania, the Regulations on the Management and Transfer of Intellectual Property of Kaunas University of Technology (hereinafter – University) and the ethical requirements stipulated by the Code of Academic Ethics of the University;

2. All the data and research results provided in the final degree project are correct and obtained legally; none of the parts of this project are plagiarised from any printed or electronic sources; all the quotations and references provided in the text of the final degree project are indicated in the list of references;

3. I have not paid anyone any monetary funds for the final degree project or the parts thereof unless required by the law;

4. I understand that in the case of any discovery of the fact of dishonesty or violation of any rights of others, the academic penalties will be imposed on me under the procedure applied at the University; I will be expelled from the University and my final degree project can be submitted to the Office of the Ombudsperson for Academic Ethics and Procedures in the examination of a possible violation of academic ethics.

Andrejus Litvakas

Confirmed electronically

Litvakas, Andrejus. Development of a Modular Radiometric Measurement System for Radiation Protection. Master's Final Degree Project / supervisor dr. Benas Gabrielis Urbonavičius; Faculty of Mathematics and Natural Sciences, Kaunas University of Technology.

Study field and area (study field group): Health Sciences, Medical Technologies.

Keywords: dosimetry, radiometry, Geiger-Mueller, open-source.

Kaunas, 2023. 59 p.

Summary

In this research a modular radiometric measurement system was developed using open-source platforms. The system was based on the RZB-04-04 dosimetry gate which was used in nuclear power plants as a personnel checkpoint. The measurement system consists of 16 *Arduino*-equipped Geiger-Mueller detector modules (each module having two SBT-10 detectors) that are capable of operating both individually and as a network.

The sensitivities of the individual detectors were analyzed using a source of ionizing radiation and calibration coefficients, required for a uniform count rate, were derived from the obtained results. The calibration coefficients for the detectors ranged from 0.8053 to 1.2686 indicating relatively good group operation quality. The 355 Volt optimal voltage required for stable operation of the detectors was determined by investigating the Geiger-Mueller (plateau) region of the detectors. Investigating 4 randomly selected modules the average deadtime of the detectors in the system was determined to be 840.413 µs. The deadtime values ranged from 284.938 µs to 1782.364 µs. Also, a conversion coefficient required for converting count rate to dose rate was derived to be 0.084 µSv/h/CPS and applied to each detector within the software.

The software developed for this system, written in *python* programming language, allows for broad further improvements and additional functionality to be implemented and employed on different platforms. The developed system offers a versatile and customizable solution for radioactivity detection and dosimetry.

Litvakas, Andrejus. Modulinės radiometrinės matavimo sistemos sukūrimas radiacinei saugai. Magistro baigiamasis projektas / vadovas doc. dr. Benas Gabrielis Urbonavičius; Kauno technologijos universitetas, matematikos ir gamtos mokslų fakultetas.

Studijų kryptis ir sritis (studijų krypčių grupė): Sveikatos mokslai, Medicinos technologijos.

Reikšminiai žodžiai: dozimetrija, radiometrija, Geigerio-Miulerio, atviras kodas

Kaunas, 2023. 59 p.

Santrauka

Šiame tyrime buvo sukurta modulinė radiometrinių matavimų sistema naudojant atvirojo kodo platformas. Sistema pagrįsta dozimetriniais vartais RZB-04-04, kurie sutinkami branduolinėse elektrinėse, kaip personalo patikros punktas. Matavimo sistemą sudarė 16 *Arduino* paremtų Geigerio ir Miulerio detektorių modulių (kiekvienas modulis turi po du SBT-10 detektorius), kurie buvo suprojektuoti veikti tiek atskirai, tiek kaip tinklas.

Naudojant etaloninį jonizuojančiosios spinduliuotės šaltinį buvo išanalizuotas atskirų detektorių jautrumas ir pagal gautus rezultatus nustatyti kalibravimo koeficientai. Detektorių kalibravimo koeficientai svyravo nuo 0,8053 iki 1,2686. Gauti koeficientai parodė santykinai gerą detektorių veikimo kokybę. Optimali 355 V įtampa, reikalinga stabiliam detektorių veikimui, buvo nustatyta ištyrus Geigerio-Miulerio (plato) detektorių sritį. Ištyrus keturis atsitiktinai pasirinktus modulius buvo nustatyta 840,413 µs vidutinė sistemos detektorių neveikos trukmė. Neveikos trukmės vertės svyravo nuo 284,938 µs iki 1782,364 µs. Taip pat buvo nustatytas 0,084 µSv/h/CPS perskaičiavimo koeficientas reikalingas detektorių skaičiavimo spartai paversti į dozės galią. Programinėje įrangoje, šis koeficientas, buvo pritaikytas kiekvienam detektoriui.

Programinei įrangai buvo panaudota *python* programavimo kalba. Programinės įrangos laisvojo kodo prieiga užtikrina galimybę ją toliau plačiai tobulinti ir naudoti įvairiose platformose.

Table of contents

List of figures **8**
List of tables **9**
Introduction **10**
1. Literature review **11**
1.1. Brief history of radiation protection 11
1.2. Overview of radiation types and their effects on human health 11
1.3. Radiation safety 13
1.3.1. Principles of radiation safety 13
1.3.2. Implementation of radiation safety 13
1.4. Dose limits 14
1.5. Importance of dosimetry in radiation protection 14
1.6. Ionizing radiation detection systems 15
1.6.1. Passive detection systems 15
1.6.2. Active detection systems 16
1.6.3. Factors affecting detection system performance 16
1.7. Geiger-Müller counters 17
1.7.1. Working principle of GM counters 18
1.7.2. Ionization chamber regions 19
1.7.3. Geiger plateau 19
1.7.4. Optimal voltage of the Geiger-Müller tube 21
1.7.5. Geiger-Müller tube efficiency 21
1.7.6. Deadtime of the Geiger-Müller tube 21
1.7.7. Advantages and disadvantages of GM counters 22
1.7.8. Dosimetry with GM Counters 23
1.8. Modular Radiometric Measurement Systems 23
1.8.1. Working Principles of Modular Radiometric Measurement Systems 24
1.8.2. Existing Modular Systems and Their Applications 24
1.9. Open-source platforms 26
1.9.1. Advantages of open-source tools in radiation detection systems 26
1.9.2. Examples of *Arduino*-based radiation detectors and dosimetry systems 26
1.9.3. Integration of GM counters with arduino microcontrollers 27
1.9.4. Performance evaluation of arduino-based GM counter systems 27
1.10. Research and development directions in radiation protection and dosimetry 28
1.11. Social impacts of open-source platforms 28
1.12. Literature review summary 29
2. Methods and materials **30**
2.1. Modular system design 30
2.2. Module operation overview 31
2.3. Optimal operating voltage determination 33
2.4. Voltage drop evaluation 33
2.5. Determination of the detector correction coefficient 34
2.6. Determination of detector deadtime 34
2.7. Determination of the dose rate conversion coefficient 35

2.8. Experimental setup 35
2.9. Software design specifications 36
3. Results 37
3.1. Determination of the Geiger plateau region 37
3.2. Voltage drop evaluation 38
3.3. Determination of detector correction coefficients 39
3.4. Determination of detector deadtime 41
3.5. Determination of the dose rate conversion coefficient 42
3.6. Software development 43
3.7. Final assembly 45
Conclusions 49
List of references 50
Appendices 56

List of figures

Fig. 1 Ionizing radiation material penetration example [11] 12
Fig. 2 Examples of various passive dosimeters [20] 15
Fig. 3 Examples of various active dosimeters [23] 16
Fig. 4 Construction of a typical GM tube [26] 17
Fig. 5 Depiction of the Townsend avalanche phenomenon [37] 18
Fig. 6 Regions of gas-filled ionization detectors [42] 19
Fig. 7 Geiger-Müller tube plateau region [45] 20
Fig. 8 Spread of secondary Townsend avalanches produced by a single incident particle [46] 20
Fig. 9 Location of RADIS monitoring stations across Lithuania [59] 25
Fig. 10 IoT based system network example 25
Fig. 11 Block diagram of a systematic data gathering and processing approach 30
Fig. 12 Block diagram of a single module (module elements enclosed in the dashed line) 31
Fig. 13 Main Arduino-equipped circuit board (left) and board standoff (right) 32
Fig. 14 Open module showing the main circuitry and detectors 32
Fig. 15 Main measurement setup 35
Fig. 16 Experimentally determined Geiger plateau region graphs 37
Fig. 17 Measured voltage drop across a range of supplied voltage graphs 38
Fig. 18 Screengrab of the developed software 43
Fig. 19 Block diagram of the basic workflow of the software 44
Fig. 20 Block diagram of the developed modular radiometric measurement system 46
Fig. 21 *ThinkCentre TIO22Gen3* monitor (left) and *ThinkCcentre M715q* computer (right) 46
Fig. 22 Component cavitity with original electronics 47
Fig. 23 *ICY BOX* USB hub (left), 5 Volt AC/DC converter (middle), component cavity (right) 47
Fig. 24 Assembled modular radiometric measurement system 48
Fig. 25 HV generator circuit diagram 58
Fig. 26 Arduino signal conditioning circuit diagram 58

List of tables

Table 1 Detector measurement results and derived calibration coefficients 40
Table 2 Detector measurement results and derived deadtime values 41
Table 3 Geiger plateau region determination measurement data..... 57

Introduction

Ionizing radiation exists both naturally and as a byproduct of human activities. It has become an increasingly important topic of study due to its potential implications for human health and safety. As our understanding of ionizing radiation has evolved, so has our ability to use it in beneficial applications, such as medical diagnostics, cancer treatment, nuclear power generation, and various industrial processes. However, these benefits come with inherent risks, necessitating the development of effective strategies for managing and controlling ionizing radiation exposure. Consequently, the field of radiation protection and dosimetry has emerged as a critical area of research, dedicated to reducing the potential hazards associated with ionizing radiation exposure while maximizing its beneficial uses.

The study of radiation protection and dosimetry is rooted in the recognition that a thorough understanding of ionizing radiation and its interactions with biological tissues is vital for the safety of human health. The history of radiation protection reflects a continuous progression in our comprehension of the risks posed by ionizing radiation exposure, as well as the development of protective measures to minimize these risks. As a multidisciplinary field, radiation protection encompasses various aspects, including the investigation of different radiation types and their effects on human health, the formulation and implementation of safety measures and guidelines, and the determination of dose limits when handling ionizing radiation sources.

The field of radiation protection has evolved alongside technological advancements, leading to the development of increasingly sophisticated detection and measurement systems. These systems have been crucial for monitoring and assessing ionizing radiation exposure, enabling researchers to better understand the characteristics of ionizing radiation and devise more effective protection strategies.

With the growing awareness of the potential hazards associated with ionizing radiation, efforts have been made to educate the public and professionals about the need for radiation protection. This has led to the establishment of regulatory bodies and the development of international standards aimed at ensuring the safe use of ionizing radiation sources in various applications. The collaboration between researchers, and regulatory agencies has been instrumental in driving the advancements in radiation protection and dosimetry, ultimately contributing to the protection of both individuals and the environment from the potential harm caused by ionizing radiation exposure.

Aim of this research work:

Develop a modular radiometric measurement system for radiation protection.

Tasks:

1. Overview currently acceptable solutions for radiation monitoring with modular measurement systems;
2. Design a single radiometry module for the modular measurement system;
3. Produce multiples of the designed radiometry module and characterize the modules;
4. Develop data analysis software and perform full system integration.

1. Literature review

1.1. Brief history of radiation protection

Radioactivity was discovered in the late 1800s when a French physicist Henri Becquerel observed photographic plates getting exposed due to their proximity to uranium salts [1]. The discovery of X-rays paved the way for Marie and Pierre Curie to identify even more radioactive materials such as radium and polonium [2]. The discovery of radioactivity was a brand new; novel, concept and soon radioactive materials were being used in everyday consumer products including toothpastes, cosmetics, and even toys [3].

Soon after the dangers of ionizing radiation became clearer. In the 20th century, scientists began to recognize both short-term and long-term dangers of exposure to this radiation, and in 1927 the first-ever death was recorded due to overexposure to X-ray radiation. [4]

In the 1920s and 1930s, the first ever radiation protection guidelines were developed in response to the concerns about ionizing radiation's effect on human health. The recommendations were based on the notion of tolerance dose. The tolerance dose referred to a level of ionizing radiation that was acceptable and relatively safe for living tissue. However, tolerance dose was later shown to be ineffective due to the fact that it did not account for long-term effects caused by ionizing radiation or the individual person's susceptibility to radiation. [5, 6]

The first international radiation protection standards and regulations were developed in the 1950s, including the establishment of the International Commission on Radiological Protection (ICRP), following the increasing use of nuclear technology in the fields of energy production and military development. The adoption of the International Basic Safety Standards for Ionizing Radiation Protection and the Safety of Radiation Sources took place in 1996. [7]

Since the discovery of ionizing radiation the radiation protection field has grown substantially and is now a multidisciplinary field that encompasses the development of safety standards, design of radiation shielding, protective equipment, as well as monitoring of ionizing radiation exposure, [7]

1.2. Overview of radiation types and their effects on human health

Ionizing radiation occurs naturally in the environment, either emanating from the soil or in the form of cosmic rays, as well as from man-made nuclear power plants, and medical devices such as X-ray tubes. [8]

The two types of radiation are ionizing and non-ionizing radiation. Non-ionizing radiation consists of the lower energy spectrum photons (up to X-rays) and lacks the energy to ionize atoms or molecules. Ionizing radiation, on the other hand, consists of higher energy photons and high-energy particles. Ionizing radiation has enough energy to ionize the atoms and molecules which in turn can cause damage to living tissue and may pose a serious threat to human health. [9]

There are 5 types of ionizing radiation [10]:

- Alpha particles;
- Beta particles;
- X-rays;

– Gamma rays;
– Neutron radiation.

Alpha particles are emitted from the nuclei of atoms, such as uranium and plutonium, undergoing the process of alpha decay in which an alpha particle (helium nucleus) is emitted. These particles lack the energy to penetrate thick materials but can be dangerous if inhaled or swallowed. Beta particles (high-energy electrons or positrons) have more energy and therefore can penetrate the body more easily than alpha particles. X-rays as well as gamma rays are high-energy photons with enough energy to penetrate many materials, including the human body, and ionize the atoms they interact with. Neutron radiation is a type that is commonly emitted during nuclear reactions. [10]

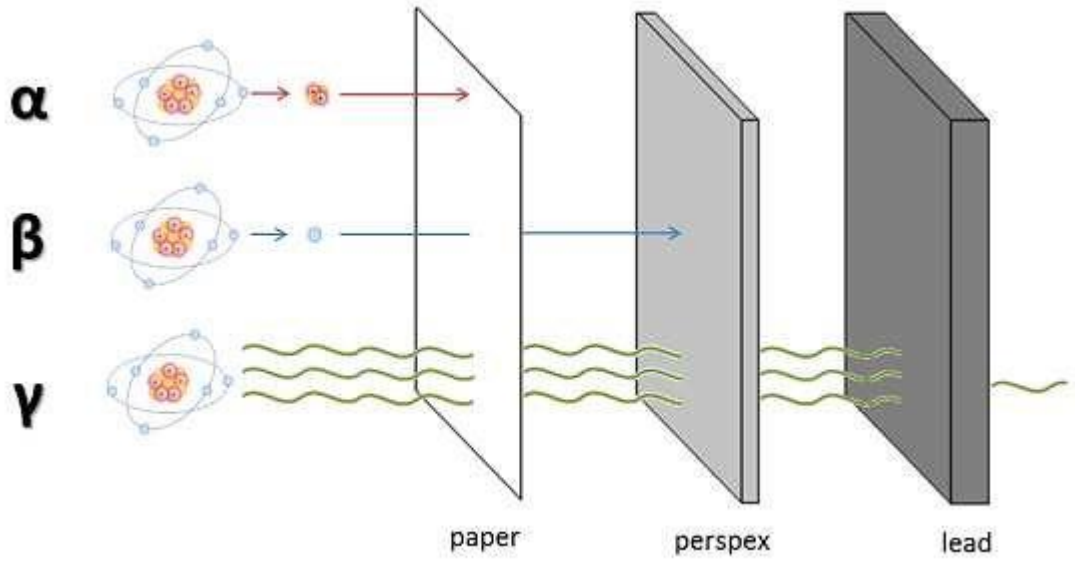

Fig. 1 Ionizing radiation material penetration example [11]

Exposure to ionizing radiation sources for a prolonged period of time or even short exposure to a strong source of ionizing radiation can have a variety of negative effects on health. Depending on the dose and exposure time the effects may include radiation sickness (which includes symptoms such as nausea, vomiting, and exhaustion), cancer, and genetic mutations. [10]

Non-ionizing radiation includes:
– Radio waves;
– Microwaves;
– Infrared radiation (IR);
– Visible light;
– Ultraviolet radiation (UV).

Even though non-ionizing radiation is far less dangerous that ionizing radiation it can still have negative health effects. For example, prolonged exposure to high amplitude (high intensity) infrared radiation may result in skin burns. Prolonged exposure to UV rays may lead to sunburn or an increased risk of skin cancer development and may accelerate skin aging effects. Some studies have even linked dangers to human health with exposure to high levels of radio frequencies emitted by phones, although the results of the studies are very inconclusive. [10]

It is critical for the public to understand the types of radiation and the potential risks associated with them. Even though not all radiation is considered harmful, only by knowing the conditions in which the radiation becomes harmful it is possible to take precautions and avoid health damage. The precautions necessary can include reducing radiation exposure, using protective gear, and following the regulations of radiation safety where sources of ionizing radiation are present.

1.3. Radiation safety

Exposure to ionizing radiation can pose severe health risks and potential dangers to the environment, therefore, radiation protection is an essential aspect of any establishment working with or in the vicinity of ionizing radiation sources. Radiation safety is primarily based on the principle of ALARA (as low as reasonably achievable). Working with radioactive sources naturally means that the personnel will get exposed to some of the ionizing radiation. While it is impossible to fully eliminate undesirable exposure, it is possible to minimize it to an acceptable level while still achieving the desired results using radioactive sources. [12]

1.3.1. Principles of radiation safety

Three basic principles exist to ensure adequate radiation safety in establishments: justification, optimization, and dose limitation.

The principle of justification is based on the weight of the benefits provided using ionizing radiation against the weight of the negative side effects or health risks. If the benefits outweigh the negatives for the individuals or environment then the use of an ionizing radiation source may be greenlit. [13]

The second principle (optimization) focuses on the reduction of undesirable exposure and uses the principles of ALARA. Minimization of unwanted exposure is achieved with the use of appropriate practices and technologies, such as shielding. The main goal of the optimization principle is to minimize the ionizing radiation exposure and maximize the potential benefits of said exposure. [13]

The dose limitation principle sets the acceptable dose limits and forces personnel, handling sources, to adhere to those limits established by regulatory authorities. The dose limits may vary based on factors such as age, occupation, and radiation type. [13]

1.3.2. Implementation of radiation safety

In order to implement proper radiation safety technical, administrative, and regulatory measures must be taken to ensure that the establishment is adhering to proper safety protocols.

Technical measures involve the enforced use of proper shielding materials, both for the personnel and for source shielding. Personnel should be equipped with proper shielding to ensure that the exposure to ionizing radiation minimizes health risks as much as possible. Source shielding involves the use of specialized containers and structures for storage of the sources when not in use. [14]

Technical measures are not enough on their own and further administrative measures have to be taken. Administrative measures involve the development of guidelines, source handling procedures, and personnel training. Furthermore, periodic audits are scheduled to ensure that the establishment is adhering to the radiation safety requirements. [14]

Finally, the regulatory measures involve the proper authorities to establish the safety standards and regulations. Regulatory authorities also, issue licenses for the possession and use of radioactive sources. [14]

By adhering to proper radiation safety principles and employing all the necessary measures to ensure proper handling and use of ionizing radiation sources, radiation safety can be ensured. As the understanding of ionizing radiation grows and new technologies emerge, the field of radiation protection must evolve and adapt in order to protect the individuals and the environment.

1.4. Dose limits

Keeping the dose limits below a certain threshold is vital to minimize potential health risk while being in the presence of ionizing radiation sources. The recommended dose limits are provided by the International Commission on Radiological Protection (ICRP) and these limits are often adapted by national regulatory authorities, although adjustments to these recommended dose limits is possible. The dose limits vary depending on factors such as age, occupation, and radiation type.

Occupational exposure dose limits are enforced on employees of establishments. The occupational dose limits provided by the ICRP recommend an effective annual dose limit of 20 millisieverts (mSv), averaged over a five-year period, with no single year exceeding 50 mSv. An equivalent dose to the lens of the eye should not exceed 150 mSv in a year. For the skin and extremities, a limit of 500 mSv per year should not be exceeded. The dose limits are different for apprentices of 16 to 18 years of age, and for students over 16 years of age. The limits for apprentices are reduced to 6 mSv for the annual effective dose, 50 mSv to the lens of the eye, and 150 mSv for extremities and skin. Pregnant workers should not exceed a dose limit of 1 mSv throughout the entire pregnancy period. The effective dose limit for students is reduced to 1 mSv annually.

Patients undergoing radiation diagnostics or treatment have no set specific dose limits as the principle of ALARA is applied to them. The doses to patients should be optimized so that the desired effect of treatments is achieved with the lowest possible exposure. Careful consideration of doses is critical when dealing with pregnant women, and children as they are more susceptible to the negative effects of ionizing radiation.

The general public has lower dose limits than employees working with nuclear materials. The recommendations provided by the ICRP for the public are an annual effective dose of 1 mSv, an annual equivalent dose to the eye lens of 15 mSv, and the equivalent dose to skin and extremities of 50 mSv per year.

1.5. Importance of dosimetry in radiation protection

To ensure the safety from ionizing radiation of employees and the public, proper dose measurements of the workplace and the environment must be made. Dosimetry plays a vital role in ensuring the health and safety of the public.

Dosimetry measures the dose from a source of ionizing radiation and can also measure the exposure to specific body parts. The information obtained through dosimetry plays a role in evaluating the conditions of workplaces and environment. Based on this data safeguards are put in place where necessary. Exposure measurements are crucial for ensuring safe working conditions in areas such as

power plants, medical facilities, and industrial workplaces where sources of ionizing radiation exist. [15]

In order to measure ionizing radiation devices, known as dosimeters are employed. There exist various types of dosimeters that include film badges, thermoluminescent dosimeters, and various electronic dosimeters. [16]

Most countries have strict regulations when it comes to radiation exposure in the workplace and to maintain a safe environment and prevent long-term health risks dosimetry not only is necessary for protection of the employees, it is also used to evaluate the establishments compliance with radiation regulations. [17]

Today a large variety of dosimeters exist, each having their benefits and drawbacks. Some of the more well known dosimeter types include film badges, thermoluminescent dosimeters (TLDs), electronic dosimeters, and ionization chambers [18]

1.6. Ionizing radiation detection systems

In medical physics, ionizing radiation detection systems are necessary for various applications such as diagnostics, radiation therapy treatments, and of course radiation protection. The detection systems measure the energy deposited by ionizing particles (alpha, beta particles) and ionizing electromagnetic radiation (X-rays, gamma rays). The main principle of the detection of deposited energy is the quantification of this energy and conversion to a measurable electrical output signal. There exist two main types of detectors – passive and active. The following subsections provide a brief overview of some of the ionizing radiation detection devices. [19]

1.6.1. Passive detection systems

Passive dosimeters are a type of dosimeter that does not utilize any external power source to collect the measured ionizing radiation Common types of passive dosimeters include film dosimeters and thermoluminescent dosimeters (TLDs).

Fig. 2 Examples of various passive dosimeters [20]

Film dosimeters are a type of passive dosimeter that uses radiosensitive emulsion to detect ionizing radiation. After ionization the emulsion changes its color (darkens) depending on the dose that it was

exposed to. This is a common dosimeter used as a personal monitoring device in medical establishments. [21, 22]

TLDs, another type of passive dosimeter, uses materials that are able to store the energy of exposure as excited states of the electrons of the material. In order to extract the dose information from TLDs, heating is required. Upon heating the material, the electrons return to their ground states and emit visible light in the process. This emitted light is then converted into electrical signals that can be interpreted as the absorbed dose. TLDs, like film dosimeters, are also used as personal dosimeters. [21, 22]

1.6.2. Active detection systems

Active dosimeters are able to provide real-time data since they rely on an external power source to either drive the detector or convert the detector signals on the spot. The two main types of active dosimeters used in medical applications are ionization chambers and semiconductor detectors. [21, 22]

Fig. 3 Examples of various active dosimeters [23]

Ionization chambers are gas-filled detectors that utilize the ionization of the gas by incident ionizing radiation to produce a current. The gas inside the chamber is some type of inert gas to ensure that no other interactions, other than incident radiation, produce a signal. The most common types of ionization chambers include proportional counters, and the Geiger-Müller counter. [21, 22]

Semiconductor detectors rely on the creation of electron-hole pairs by incident radiation in the material that generate a current. The materials often used in this type of detector are silicon diodes and cadmium telluride (CdTe). These detectors provide high sensitivity and high energy, because of this they are often used in diagnostic radiology, nuclear medicine, and radiation therapy. [21, 22]

1.6.3. Factors affecting detection system performance

Performance of detection systems may be affected by various factors both internal and external. Several factors affecting performance are sensitivity and resolution, the linear energy transfer (LET), and environmental conditions. [24]

The sensitivity and resolution are dictated either by the construction of the detector itself or by the signal interpreting hardware or software. When measuring low doses of ionizing radiation, it is recommended to choose a detector with a high enough sensitivity and high resolution. [24]

Different detectors are better suited for radiation with different linear energy transfers. Ionization chambers for example, are suitable for detecting lower LET radiation such as X-rays and gamma rays, and detectors that use semiconductor electron-hole pair generation can be suitable for both high and low LET alpha particles. [24]

Environmental conditions such as temperature, humidity, and pressure may also affect the performance of detectors in various ways. Since the operating conditions may greatly differ from location to location and even day to day, proper instrument calibration is required to ensure reliable measurements under different conditions. [24]

1.7. Geiger-Müller counters

The original gas-filled ionizing radiation detector was invented in 1908 by the German physicist Johannes Wilhelm "Hans" Geiger. Sometime later in 1928 the original detector was improved with the help of Walther Müller and this detector today is known as the Geiger-Müller (GM) counter. The GM counter utilizes a gas-filled chamber to detect ionizing particles that pass through the gas. The invention of the GM counter has revolutionized the radiation detection methods by providing a more reliable and accurate way of detecting radioactivity, and to this day the counter persists to be one of the most popular choices for the detection of ionizing radiation, being employed in fields such as medicine, nuclear power, and environmental monitoring. [25]

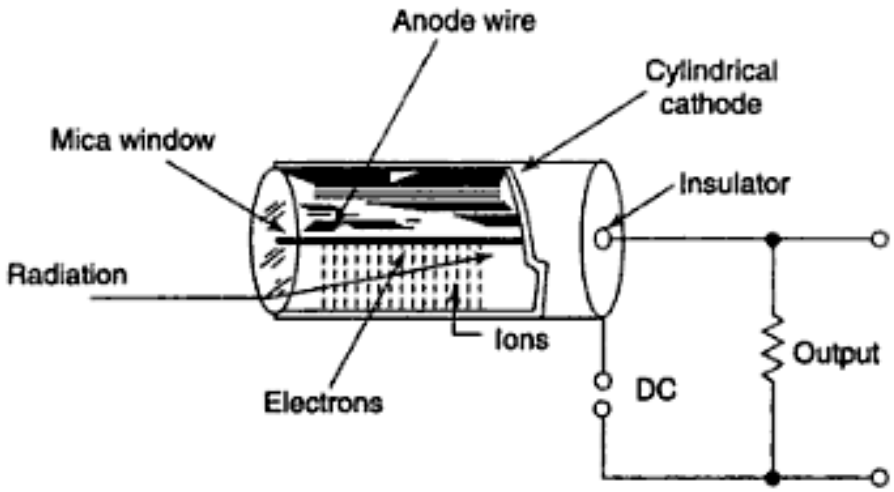

Fig. 4 Construction of a typical GM tube [26]

The GM counter differs from its counterpart, the proportional counter (also an ionization chamber detector), by employing the electron avalanche effect (also known as Townsend avalanche). During this avalanche of free electrons, the initial signal is greatly amplified before being registered by the detection circuitry. Due to this avalanche effect the ionization of the inner gas is independent of the initial incident particles energy. [25, 27]

Radiation protection instruments, including active personal dosimeters [28], and area monitors [29], frequently use GM counters. The counters are also widely used in various early-warning network applications [30] and to this day are the focus of ongoing research and development. [31]

1.7.1. Working principle of GM counters

GM counters operate on by detecting ionization caused by the ionizing radiation inside the chamber. The tube itself is relatively simple in design and consists of a gal filled chamber with the outer walls acting as the negative terminal (cathode) and an inner wire acting as a positive terminal (anode). Usually around 300-500 Volts of DC current (depending on the construction of the tube) is applied to the terminals. The voltage of the tube should be kept sufficiently close to the breakdown voltage of the inner gas. This is required to maintain a strong electric field inside the chamber. The voltage applied cannot exceed the gas breakdown voltage since that would cause the gas to ionize without any incident radiation. [32]

When a particle of ionizing radiation enters the chamber it interacts with the gas atoms, transferring some or all of its energy giving the electron of the atom enough energy to overcome the Coulomb forces that bind it to the nucleus allowing it to escape. This free electron is attracted to the anode of the chamber and as it moves through the gas it interacts with other atoms of the gas. The acceleration due to the high electric fields gives the free electrons enough energy to ionize more atoms, creating even more free electrons. These additional freed electrons also can cause more ionization. A single particle of ionizing radiation causes an avalanche effect, also known as Townsend avalanche. [33]

This avalanche of electrons produces a pulse signal that is registered by the GM counters circuitry. A single pulse corresponds to a single ionizing particle. Due to the avalanche phenomenon the pulse strength is not proportional to the energy of the incident particle. This amplification of the initial signal makes the GM counter a highly sensitive detector. [34–36]

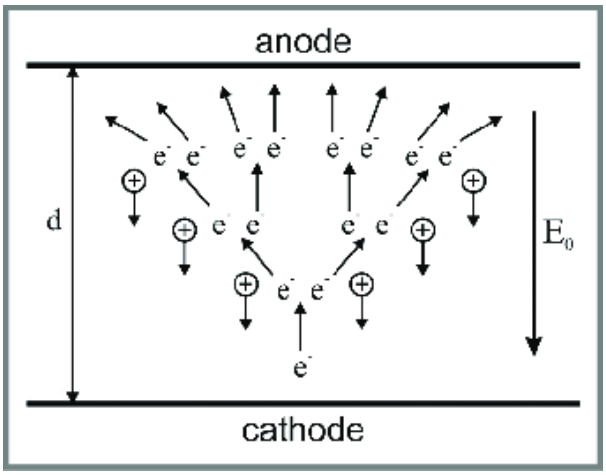

Fig. 5 Depiction of the Townsend avalanche phenomenon [37]

The pulses produced by the avalanche effect reach around 10 μV. The amplification circuitry then amplifies this pulse signal to around 5 – 50 Volts and passes it on to the rest of the processing circuitry. Since the pulse produced corresponds to a single particle of ionizing radiation, the GM counter outputs the readings in counts per unit time by default. By knowing the parameters such as type of gas used in the chamber, the volume of the chamber and other variables it is possible to determine a

conversion factor (usually provided by the manufacturer). This conversion factor can then be used to convert the counts per unit time to dose rate. [38, 39]

The ionization also produces positive ions that are attracted towards the cathode where the recombination process takes place, returning the positive ions to a neutral state. [40]

1.7.2. Ionization chamber regions

Ionization chambers come in different designs and constructions. Some may have a design where the output of the detector (pulse strength) is proportional to the energy of incident particles. Such is the design of the proportional counter. The design of a GM counter for example does not yield a proportional output. One of the main factors, along with gas type, pressure, and overall design, affecting the pulse height and proportionality is the applied voltage. There are six main regions of applied voltage that determines the behavior of the detector. Out of the six regions there are three regions that are particularly useful for ionization chambers, these regions are [41]:

- Ionization region;
- Proportional region;
- Geiger-Müller (plateau) region.

Fig. 6 illustrates the different voltage areas for alpha, beta, and gamma radiation.

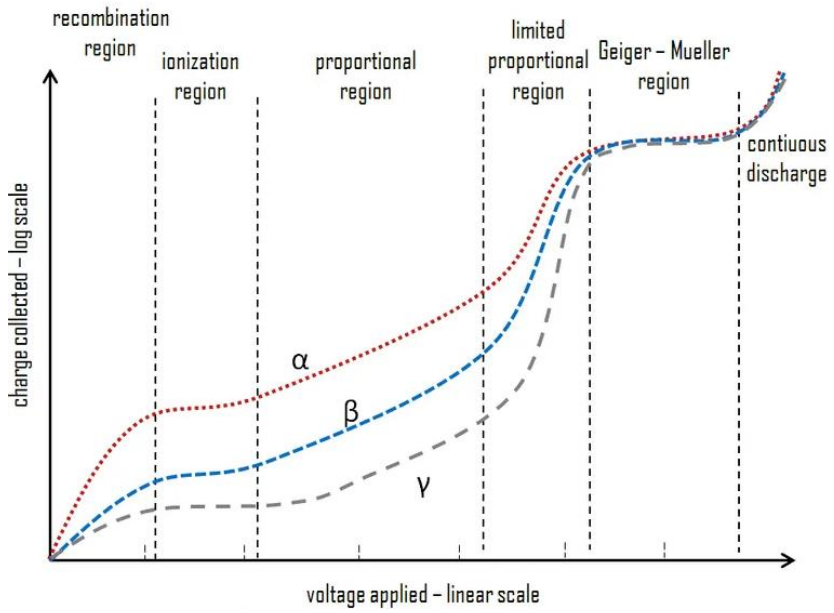

Fig. 6 Regions of gas-filled ionization detectors [42]

The graph shows three curves for three different ionizing radiation types. Each type generates a different amount of ion pairs in the recombination region, therefore, shifting the curve up or down. The alpha curve generates the most pairs and is higher than the beta and gamma curves. This difference in ion pair generation continues up to a portion of the limited proportionality region and upon reaching the plateau region effectively equals out. [41]

1.7.3. Geiger plateau

In order for the GM counter to function, it has to operate in a specific voltage range defined by the construction of the tube. Each GM counter type will have a different operating voltage range. Usually,

the voltage range for operation is from 300 V to 500 V. If the applied voltage to the tube is to low the detector will not register any counts, and if the voltage is set to high, exceeding the gas breakdown voltage, then a continuous discharge will occur and the detector will essentially short circuit. [43, 44]

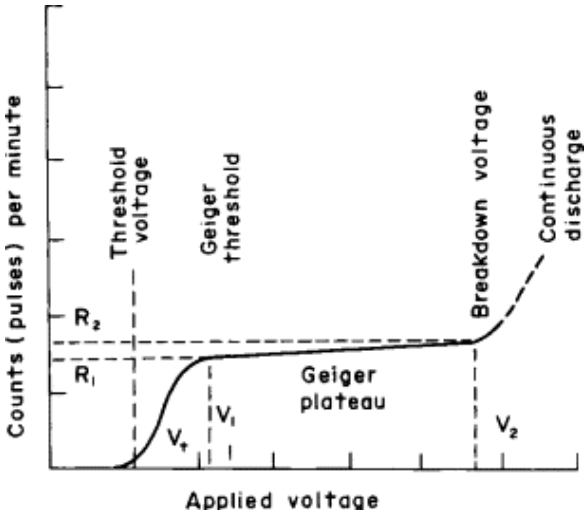

Fig. 7 Geiger-Müller tube plateau region [45]

The Geiger plateau region defines the operating range of the detector. In this region the count rate of the detector is not related to the applied voltage. Due to the intense electric fields generated in this region secondary electron avalanches can occur. The secondary avalanches can be generated by photons emitted by atoms from the initial avalanche, spreading through the entire tube, meaning that the entire chamber can get ionized. [45]

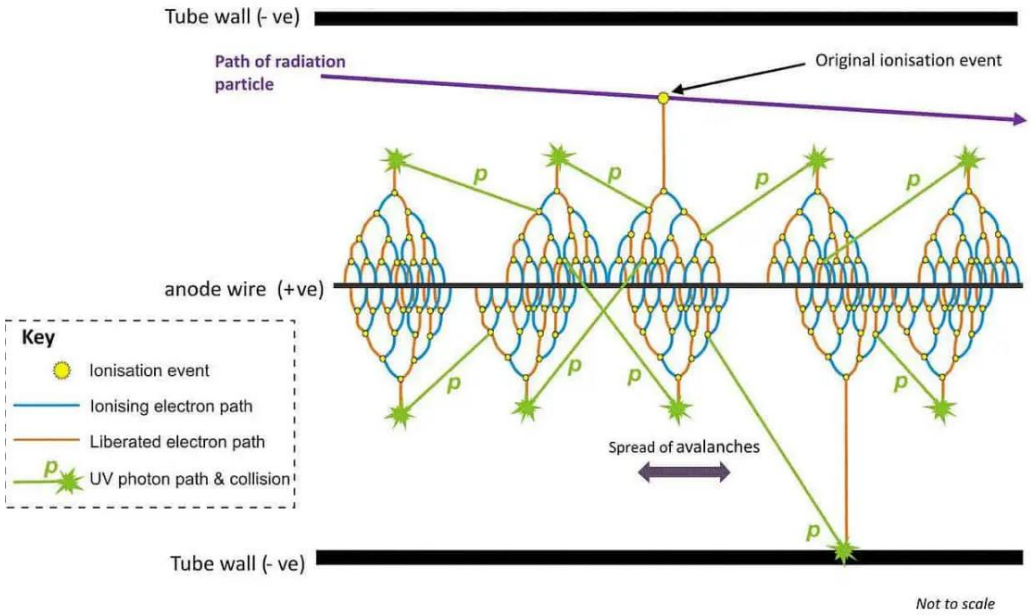

Fig. 8 Spread of secondary Townsend avalanches produced by a single incident particle [46]

These avalanches amplify the initial photon signal, and this amplification factor can reach a factor of 10^{10}. Detectors operating in the plateau region can detect X-rays, gamma rays and any charged particles that can reach the detector. [47]

1.7.4. Optimal voltage of the Geiger-Müller tube

As mentioned previously the voltage range of the plateau region is not the same for all GM detectors. The voltage range can be experimentally determined using a simple methodology. Initially the voltage applied to the detector must be low enough for the detector to nor register any counts. Using a source of ionizing radiation set up near the detector the applied voltage should be gradually increased by a defined voltage step. After a specified amount of time, at each voltage step the measurement should be noted. Repeating the step multiple times for each voltage increment and plotting the data on a graph (count rate versus voltage) gives a curve of the plateau region. By determining the part of the curve with the lowest derivative we can obtain the optimal operating voltage of the detector. [19]

1.7.5. Geiger-Müller tube efficiency

The efficiency of the GM counter depends on the incident ionizing radiation and the construction of the tube. Alpha particles are highly attenuated by the tube window material therefore the efficiency will depend on the window material as well as the distance to the radiation source. Alpha particles have less than around 50 mm of free mean path in air, meaning that the farther away from the source the detector is located the less efficient it is in measuring the source activity. It is recommended to have the window material have a density of 1.5-2.0 mg/cm² to achieve a compromise between attenuation and efficiency. GM counters constructed with narrow windows are ideal for high-energy beta particles, however, when the energy of the beta particles decreases the window material starts playing a role in attenuation, lowering the tube efficiency. For high energy photons (gamma, and X-rays over 25 keV) the atomic number of the tube wall material plays a big role. [48]

1.7.6. Deadtime of the Geiger-Müller tube

The process of ionization and recombination is not instantaneous, meaning that it takes a certain amount of time for the inner gas of the detector to return to a neutral state. The time it takes for the detector to return to a neutral state is called deadtime (sometimes called recovery time). It is the time period during which the GM counter is unable to register any new ionization events. It is vital to know the deadtime of the detector when measuring high activity sources. If the activity of the source exceeds the deadtime period the GM counter will not be able to register all of the incoming high energy particles and will readout a lower value than it actually is. A detector with a very large deadtime may output readings that indicate that the environment is safe and does not pose any health risks when, in reality it is unable to keep up with the bombardment of high energy particles. Understanding deadtime not only is useful for accurate measurements but also critical for health risk assessment. The deadtime of the detector depends on several factors such as volume of the chamber, chamber shape, and the inner gas mixture. Usually, deadtime can range from a few microseconds for smaller chambers and over 1000 microseconds for large volume chambers. [49]

Deadtime can be measured using a few different methods such as SCA (single channel analyzer) and two-photon polymerization methods. The SCA method consists of gradually increasing the activity and measuring the count rate. Activity may be increased by either using additional sources or by relocating the source closer to the detector since the activity of the source is linked to the inverse square law. Eventually the count rate reaches a saturation point where the rate does not increase any further. This point where the counts do not increase is the detectors maximum count rate, out of which deadtime may be calculated. [50]

Two-source method involves the use of two sources of radioactivity. By measuring the count rate of the single source and measuring the rate of two sources, the deadtime can be calculated.

It is possible to determine the deadtime of the detector using two sources of ionizing radiation. Each individual count is associated with a deadtime (τ). The total GM tube deadtime (T_{dead}) may be expressed by measuring the count rate (r) over a period of time (Δt) [51]:

$$T_{dead} = (r\Delta t)\tau \tag{1}$$

The true counting rate (R) of the detector is related to the measured count rate $r = R(\Delta t - T_{dead})$. Rearranging the equation and expressing the true count rate we get [51]:

$$R = \frac{r}{1 - r\tau} \tag{2}$$

Using two sources of ionizing radiation it is possible to determine the deadtime by measuring the count rate using a single source and the count rate of the two combined sources. It follows that the combined count rate (R_c) should be equal to the sum of individual count rates (R_1 + R_2). We can arrange the equation in the following manner [51]:

$$\frac{r_c}{1 - r_c\tau} = \frac{r_1}{1 - r_1\tau} + \frac{r_2}{1 - r_2\tau} \tag{3}$$

Expressing the deadtime (τ) from equation (3) gives us the deadtime [51]:

$$\tau = \frac{r_1 + r_2 - r_c}{2r_1r_2} \tag{4}$$

Improper determination of the detector deadtime may result in substantial measurement errors and therefore the methodology to determine the deadtime should be devised very carefully for accurate determination of the deadtime.

1.7.7. Advantages and disadvantages of GM counters

The Geiger-Müller counter is a popular choice for radioactivity monitoring due to its several advantages over other detectors [52]:

- Fast response time
- Real-time count rate and/or dose rate
- Portability and ease of use, making them ideal for field operation
- Wide dynamic range, allowing to measure both high and low rates
- Relatively inexpensive

Overall, these benefits make GM counters a good choice for radiation detection in various fields including medical physics, nuclear power plants, environmental monitoring applications. However, despite their advantages, GM counters also come with disadvantages [52]:

- Limited accuracy and precision at low dose rates;
- Only measure external radiation exposure;
- Sensitive to environmental factors such as temperature and humidity;
- Inability to distinguish energy levels of incident particles;
- Dose rates are only approximated.

The inability to differentiate between different particle energy levels is a major disadvantage of a GM counter. Furthermore, GM counters cannot provide accurate dose rate information. Since the GM counter is calibrated using a specific ionizing radiation source it can get tricky to determine the actual radiation dose rate from other sources of ionizing radiation. For example, trying to determine the dose rate from a cobalt-60 source using a counter calibrated with a cesium-137 standard will give only half of the actual dose rate value. This is due to cobalt-60 having twice the energy of cesium-137. On the other hand, measuring radionuclide activity of lower energies than cesium-137 will yield a reading of a higher dosage. In, general a simple GM counter is not best suited for accurate dose measurements. A GM tube can only measure the exact dose of the radionuclide it was calibrated with. [52]

1.7.8. Dosimetry with GM Counters

GM counters are employed in the field due to their ease of operation, fast response times, and accuracy and can act as both radioactivity detectors as well as dosimeters for dose rate determination.

To be used as dosimeters GM counters must be properly calibrated with a reliable source of ionizing radiation with a known dose rate at a chosen distance from the measuring point. After calibration the readings of the counter should be verified by a second reliable detector. The estimation of the dose rate requires the correct proximity to the source of ionizing radiation. The method by which the count rate is converted to dose rate is the application of a conversion coefficient (CF). The datasheets of GM counters usually provide the sensitivity to the gamma ray energy the detector was calibrated with. This sensitivity is usually written in the form of counts per unit time per dose rate, for example, CPS/µSv/h. Using this sensitivity, it is possible to derive a conversion coefficient for a single count per unit time. Then the conversion coefficient can be applied to the detectors count rate to obtain a dose rate value. [53]

GM counters are commonly used for dosimetry in a variety of applications, including radiation monitoring of nuclear power plants and medical facilities, environmental monitoring of radioactive materials, personal dosimetry for personnel, and emergency response to radiation incidents. [54]

1.8. Modular Radiometric Measurement Systems

Modular radiometric systems are systems designed to be scalable and highly customizable. The systems are composed of multiple independent components or modules. The modules are designed to work independently as well as in a network of multiple modules. This modularity and scalability of these systems allows great flexibility and customization in term of both functionality and configuration. Modular measurement systems can be tailored to multiple use cases such as area monitoring, personnel dosimetry, and both mobile and static environmental monitoring. [55]

The main benefits of a modular radiometric system are:

- Flexibility;
- Scalability;
- Ease of maintenance;
- Cost-effectiveness.

The scalability of the systems may be more cost-effective than a standard all-in-one solution by selecting only the most necessary components. Even the most basic modular systems have much

better solutions of upgradability due to the modular nature, allowing for more modules to be added if necessary, giving them a high adaptability to the required applications. [55]

1.8.1. Working Principles of Modular Radiometric Measurement Systems

The working principle of a modular system man vary from system to system depending on the specific design. Nevertheless, most of the modular systems follow the basic, systematic operating approach that involves the detection of radiation, generation of a signal, signal processing, data acquisition, and data analysis. [56]

The first step of any radiometric system is the detection of radiation. The method of detecting the ionizing radiation varies based on the choice of the detector for the specific application. Common types of detectors in such systems include gas-filled detectors (GM or proportional counters), scintillation detectors, or semiconductor detectors. [56]

After the detection of ionizing radiation, the next step is to generate a signal. The signal generation is usually incorporated into the detector itself. The raw signals generated by the detectors may be too weak for adequate processing and may require amplification. The processing modules may consist of preamplifiers, amplifiers, and filters that help with the readability of the signal by amplifying, de-noising, and shaping the signal. The signal processing stage extracts the useful information from the signal such as pulse height, pulse shape, etc. [56]

The amplified and shaped signal then reaches the data acquisition stage where the signals are digitized using analog-to-digital converters (ADCs). These digitized signals can then be either stored or sent out for further analysis. The analysis of the signals is the final stage of the system where all of the gathered data is analyzed by a dedicated software to output meaningful data such as dose rates, activity, or energy spectra. [56]

1.8.2. Existing Modular Systems and Their Applications

There exist multiple modular radiometric systems that are currently deployed in the field on varying scales. Modular systems may be deployed locally, nationally, or even at a global scale. Examples of the currently deployed modular systems on different scales are the RadNet, SAUNA, and RADIS systems as well as the Internet of Things-based radiation monitoring systems. [57–59]

The RadNet environmental monitoring system is located in the United Kingdom and is operated by the Environmental Protection Agency (EPA). RadNet is composed of multiple different components both static, and deployable. The components include gamma detectors, air samplers, and meteorological sensors. The purpose of RadNet is to continuously monitor radioactivity levels in the environment. [58]

The Swedish Automatic Unit for Noble Gas Acquisition (SAUNA) is a modular system developed by the Swedish Defense Research Agency (FOI). Its purpose is to monitor the concentrations of noble gasses (particularly xenon) in the atmosphere for the purposes of verifying the compliance of the nuclear test ban treaties. SAUNA is part of the global International Monitoring System (IMS), overseed by the CTBTO (Comprehensive Nuclear-Test-Ban Treaty Organization). [57]

RADIS (RADiation Information System) is a Lithuanian national environmental monitoring system that continuously measures the levels of gamma radiation in the environment. The system is

composed of remote monitoring stations each capable of transmitting data to a central processing unit that handles real-time data analysis. The RADIS system is used as an early warning system in the event of a radiological incident. The stations (modules) of the RADIS system are scattered across the country. The location of the individual stations can be seen in **Fig. 9**. [59]

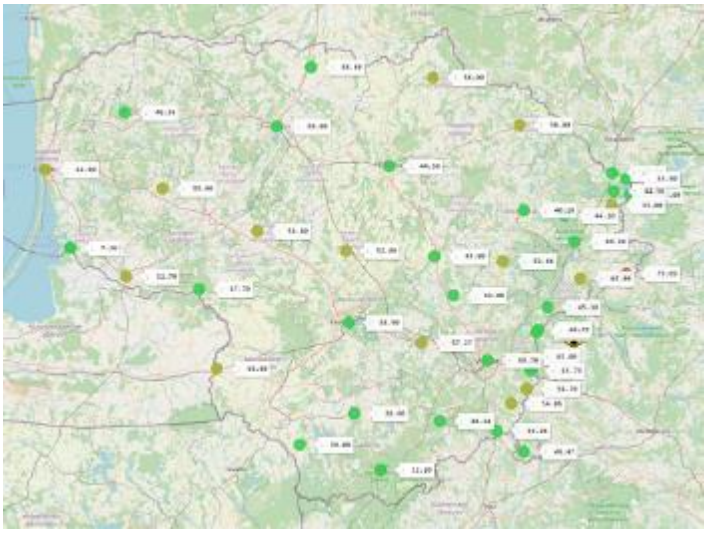

Fig. 9 Location of RADIS monitoring stations across Lithuania [59]

Internet of Things (IoT)-based monitoring systems utilize the IoT technology. These systems differ from other modular systems in essence by internet connectivity. The modules are able to communicate over the internet as well as send data wirelessly. IoT based systems offer better scalability since additional devices only need to connect to the internet-based system, no physical connections to the system are necessary.

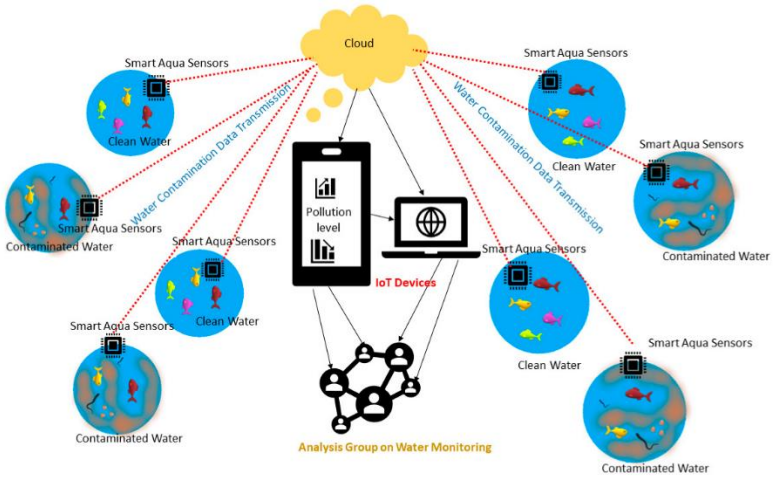

Fig. 10 IoT based system network example

The cloud-based architecture of the system essentially allows anyone and anywhere to be part of the data network. In terms of processing power regular modular systems are limited by the processing unit of the system. An IoT based system can use cloud-based computing and analysis, as well as employ machine learning capabilities. Due to the nature of the system security of the data becomes a concern. Proper measures should be taken to protect the data. The required security measures include

data encryption, authentication methods, and regular software security updates. Overall, the IoT based system are possibly the most flexible of all modular systems. [55]

The above-mentioned systems demonstrate the flexibility, versatility, and capabilities of modular systems. As technology advances further these systems will undergo even more advancements in development and capabilities, step by step turning them into the most sophisticated and versatile detection systems.

1.9. Open-source platforms

Open-source platforms refer to software and tools that are openly available to the public. Open-source software can be cost-effective and highly customizable. A few examples of open-source platforms include *PyNE*, *Geant4*, and *Arduino*.

PyNE (Python for Nuclear Engineering): a library of tools designed for ionizing radiation detection, data analysis, and modeling [60]. *Geant4* is a *C++* toolkit designed for simulating the passage of particles through matter. This toolkit is often used in particle physics and radiation detection and is useful for development of complex detector systems [61].

Arduino is an open-source electronics platform of various available *Arduino* hardware components. It is used for building interactive electronics projects that utilize the *Arduino* microcontroller. The microcontroller is a programmable chip capable of handling interactions between the physical hardware and software of the project. [62]

1.9.1. Advantages of open-source tools in radiation detection systems

There are many benefits of using open-source tools in radiation protection systems. Open-source systems provide very high customizability due to the nature of open-source code. Since the source code of the software is openly available to the public, the user is free to make any necessary adjustments to the code, and even add new functionality to existing software. Furthermore, open-source projects usually have a large and diverse community of both professionals and enthusiasts in collaboration, leading to rapid improvements on the software. [63]

Open-source projects offer transparency and trust due to the usually large community of the project. This ensures the absence of any malware that may be hidden in the code, as users that use and work on the software would spot any malicious code in the project. Finally open-source projects offer a great educational value. Students or simple enthusiasts are able to get a hands-on experience with real-life applications of the field they are interested in, without having to purchase any proprietary software. [64]

1.9.2. Examples of *Arduino*-based radiation detectors and dosimetry systems

In order to develop and customize open-source projects usually multidisciplinary knowledge is required. Not only is it required to be knowledgeable in the field for which the project is being developed, but also some understanding of software development and even electronics engineering is desired. Nevertheless, there are many experts and enthusiasts alike that are developing open-source projects. Some examples of open-source projects that can be used for radiation safety systems are [65–67]:

- Open-Source Radiation Detector (*OSRaD*) is a low-cost ionizing radiation detection system based on the Geiger-Müller counter and open-source electronics platforms such as Arduino or Raspberry Pi boards. The boards are used for data acquisition and processing;
- *uRadMonitor* is a global network of monitoring stations that are internet-based and open-source. The stations use various detectors to collect data about environmental radiation levels, process the data and make the processed data available online for public access. This open-source system helps to contribute a better worldwide understanding of ionizing radiation;
- *PENELOPE* (Penetration and ENErgy LOss of Positrons and Electrons) is an open-source code that uses the Monte Carlo method to simulate the transport of photons, electrons, and positrons in materials. The code can be used alongside ionizing radiation detectors to simulate the interactions of ionizing radiation with matter and estimate dose distributions.

Open-source projects can have various applications ranging from environmental monitoring to medical imaging and radiation safety systems.

1.9.3. Integration of GM counters with arduino microcontrollers

Integrating the Geiger-Müller counter with an *Arduino* board (or similar microprocessor boards) comes with certain challenges. One of the challenges is the fact that a GM, depending on design, can operate anywhere from 300 – 900 V. *Arduino* boards operate at much lower voltages (3.3 or 5 Volts). This voltage must be stepped-up using a high voltage (HV) generation circuit. Alternatively, an external HV power supply may be used. [53]

The signal produced in the GM tube is not properly conditioned for accurate processing by the *Arduino* so an additional signal conditioning circuit should be used. Signal conditioning can be performed by employing a comparator circuit or a Schmitt trigger circuit to convert the signal into a clean pulse that is compatible with the *Arduino* digital input pins. [53]

Finally, noise reduction is necessary to ensure proper readings. Electrical noise can cause false signals to be registered. While designing the circuitry proper shielding, grounding, and filtering must take place to eliminate as much unwanted signal noise as possible. Additionally, the use of interrupt-driven pulse counting methods can help improve the pulse detection accuracy. [53]

1.9.4. Performance evaluation of arduino-based GM counter systems

As with any DIY (do-it-yourself) project, the performance of the finished product must be evaluated. Performance evaluation may include evaluating the detection efficiency, count rate stability, and overall measurement accuracy. [53]

The detection efficiency can be assessed by exposing the GM counter to a radioactive source of known activity. Comparing the theoretical count rate to the measured count rate the efficiency can be evaluated. The stability of the count rate can be tested by monitoring the performance of the detector over a prolonged period of time and determining the percentage of deviation from the average count rate. Finally, the measurement accuracy can be determined by comparing the DIY GM detectors readings with the readings of a reliable, properly calibrated detector. [53]

1.10. Research and development directions in radiation protection and dosimetry

The future prospects in radiation detection and measurement technologies are limitless. With the advancements in fields such as material sciences, new materials may be developed to help improve the detection and performance of the detector systems. Advancements in machine learning and artificial intelligence may accelerate the analysis of datasets. As most technology is heading towards miniaturization, the development of more compact and portable systems may be possible. Also, with the rapid growth of the internet-of-things, cloud-based systems may be adopted for more efficient data analysis using cloud-computing. [68, 69]

It is expected that with the advancements of technology, modular detection systems may benefit from new materials and miniaturization to enhance the flexibility and scalability. Incorporating the ever-growing field of robotics into ionizing radiation detection systems could reduce human exposure in hazardous environments. Research and development are necessary in the field of radiation protection due to the increasing use of nuclear technologies and the associated radiological incidents. [68, 69]

Since ionizing radiation is invisible and the negative health effects are not always immediate, there may be people that take radiation safety dangerously lightly. Public safety from the negative effects of ionizing radiation relies on proper public awareness and education on the possible hazards of exposure [70]. Open-source systems may provide an opportunity to educate the public about ionizing radiation by shedding light into the inner workings and procedures of ionizing radiation detection and safety measures.

1.11. Social impacts of open-source platforms

The development of an open-source radiometric measuring system for radiation protection may have broad impact on society. The open-source model promotes inclusion by allowing people from all backgrounds and incomes to participate in the creation, modification, and usage of such technologies [71]. This might lead to democratization of technology access and promote innovation [72]. Furthermore, the incorporation of these systems into the larger Internet of Things (IoT) network opens up new opportunities for customized radiation monitoring. This might result in a greater sense of personal responsibility for radiation safety and the preservation of the environment. It does, however, present the challenge of ensuring data security and privacy [72]. The implementation of such open-source systems has the potential to improve science literacy by providing practical and interactive learning platforms. Open-source systems have the ability to bridge the gap between the scientific community and the general public, thus increasing public trust in research. However, there is a need to reduce the risks of misinterpretation and misinformation by providing enough educational resources and clear communication regarding the data provided by these systems [73].

Delving deeper into the social implications, an open-source radiometric measuring system represents a paradigm shift in the distribution of scientific information and technology [72]. Access to such tools has historically been restricted to specialized institutions or occupations. The open-source model encourages a more diffused type of scientific collaboration by breaking this paradigm [72]. As individuals are provided with the knowledge and information required to independently assess ionizing radiation dangers and protect their environment, this could lead to a shift in society toward a more educated and proactive population.

Finally, widespread use of open-source radiometric measurement equipment may increase public interest in scientific research. Such interest, promoted by readily available and practical educational tools, might lead to an increase in science literacy, resulting in a society that is more equipped to understand and take part in scientific discussions and decisions [74]. Nonetheless, carefully curated training resources are required to guarantee that the data provided by these systems is appropriately analyzed and that possible ionizing radiation risks are correctly recognized [73]. As a result, developing an open-source system involves a complex interplay of benefits and challenges requiring meticulous planning and implementation.

1.12. Literature review summary

Radiation protection has evolved significantly over time, from early observations of the biological effects of ionizing radiation and progressing to the establishment of dose limits, safety measures, and modern dosimetry.

Ionizing radiation poses risks to human health, necessitating the development of various radiation detection systems. Passive and active systems aid in the measurement and monitoring of ionizing radiation exposure. Geiger-Müller (GM) counters are widely used due to their versatility and performance. They operate through the detection of ionization events within a gas-filled chamber and exhibit unique characteristics, such as the Geiger plateau and deadtime.

Modular radiometric measurements systems provide a way for area monitoring in contrast to single unit dosimeters or radiometers. Open-source platforms have emerged as a valuable tool in radiation detection, with *Arduino* or similar open-source hardware-based systems gaining traction for their flexibility, affordability, and ease of integration with existing technologies like GM counters. Continued research and development in radiation protection and dosimetry strive to enhance existing systems and develop new, innovative technologies that promote safety and accurate measurement of ionizing radiation exposure.

2. Methods and materials

The modular radiometric measurement system was designed based on the soviet *RZB-04-04* (*РЗБ-04-04*) dosimetry gate, that was used in nuclear power plants as checkpoints for determining the contamination levels of employees. Originally the dosimetry gate would measure the full body contamination levels of personnel and issue a pass or fail signal, meaning that the system was binary and would not read out any detailed information about the registered activity or dose rate.

This project focuses on the redesign of the functionality of this dosimetry gate and aims to provide the user with relevant, accurate, and detailed information about the registered activity and dose rate.

2.1. Modular system design

The modular system was designed to follow the basic systematic data gathering and processing approach as depicted in the block diagram (**Fig. 11**).

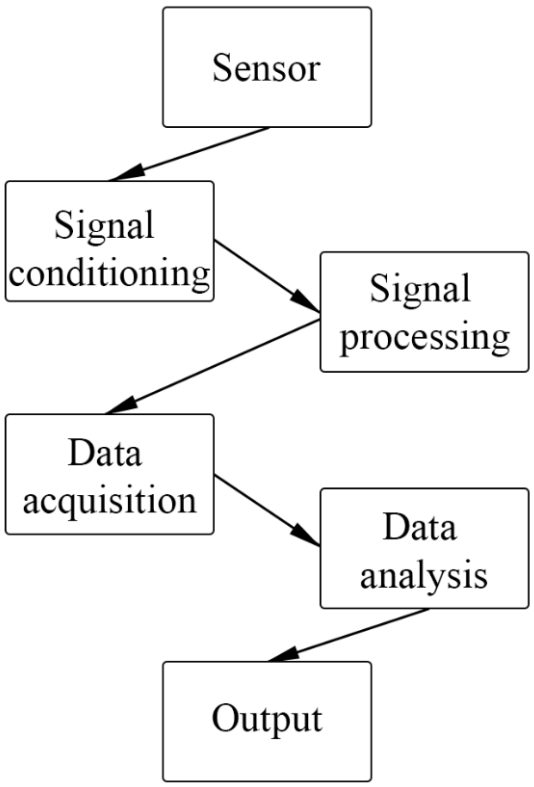

Fig. 11 Block diagram of a systematic data gathering and processing approach

The system design used 16 detection modules in total. The overall design should take into account the modularity of the system and be able to function with a single module as well as with all of the modules without any loss of functionality or overall system stability. A design choice was made to build custom circuitry based around the *Arduino* microcontroller with a goal of creating a module capable of high voltage generation required for the operation of GM tubes, signal conditioning and processing, and data acquisition (conversion of analog signals to digital signals).

The data acquired by the modules should then be transmitted to a central analysis system, or a mainframe. The collected data would then be analyzed and/or stored by the dedicated software.

2.2. Module operation overview

The redesigned modules omitted almost all of the original electronics components and were equipped with custom built components, including an *Arduino* equipped main circuit board and custom 3-D printed standoffs for holding the components. The working principle of a single module is shown in the block diagram (**Fig. 12**).

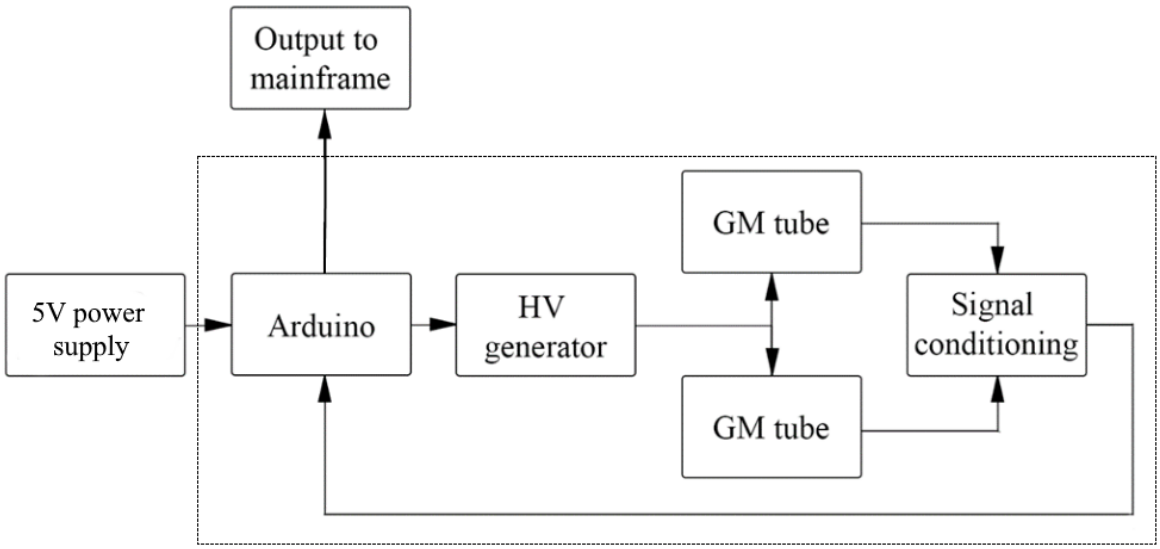

Fig. 12 Block diagram of a single module (module elements enclosed in the dashed line)

Each module was equipped with two *SBT-10* (*СБТ-10*) square chamber GM tube detectors. Having two detectors in a single module posed a question of the HV generation circuit functionality. If the HV circuit would be poorly designed there could be a potential for a large voltage drop caused by one of the detectors upon registering an ionization event. Each event essentially produces a short circuit in the GM tube causing the operating voltage to drop slightly. This may lead to the second detector not being supplied by enough voltage to register an event during the time it takes the supply voltage to return to its set value. The HV generation circuit was tested prior to final assembly and no significant voltage drops were observed.

5 Volts are supplied to the *Arduino* microcontroller which the transmits this voltage into the HV generation circuit. The HV generation circuit steps up the voltage to the value required by the GM tubes. The single HV generation circuit provides high-voltage to both detectors. After registering an ionization event, the GM tubes then transmit a signal to the signal conditioning circuit which transmits the conditioned signal to the *Arduino* microcontroller. The microcontroller then accumulates the number of counts it received over a time period of 1 second and transmits this data to the mainframe (computer equipped with the analysis software). Each *Arduino* in a module was programmed with an identification code that would allow the software to know from which module the data came from.

An example of the main circuit board along with the 3-D printed support structures can be seen in **Fig. 13**. The standoffs were designed in such a way that the main circuit board would rest in the center cut-out slots of the standoffs. Each module was equipped with two standoffs to support the main circuit board from both sides. For further security of the main board, the standoffs were designed to be pressed down with the cover of the module which prevented any movement of the main circuit board. Furthermore, this design prevented any contact with the aluminum casing of the module,

preventing any possible short circuits that may cause the board to malfunction. The inner components of a functioning module are shown in **Fig. 14**.

Fig. 13 Main Arduino-equipped circuit board (left) and board standoff (right)

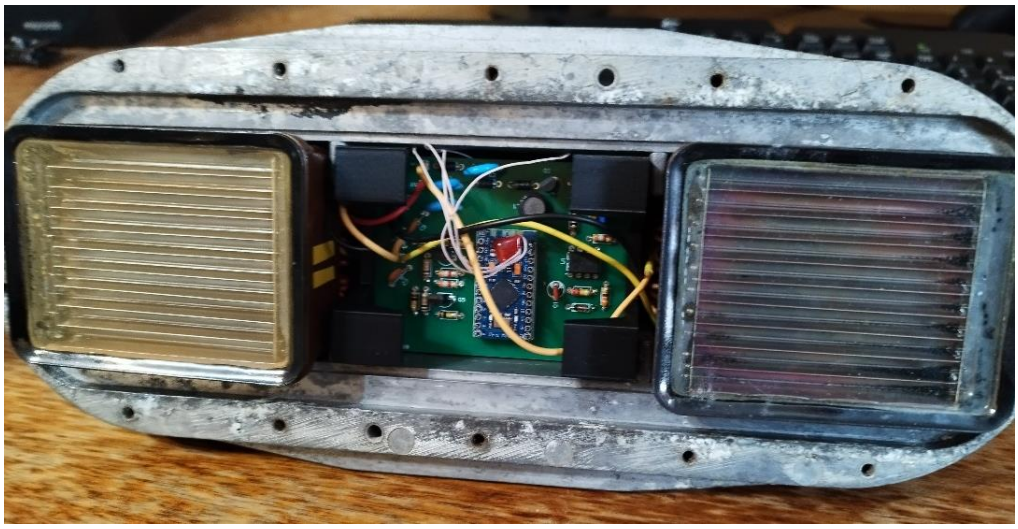

Fig. 14 Open module showing the main circuitry and detectors

For optimal performance several key parameters of the modules had to be evaluated:

- Optimal operating voltage
- Evaluation of voltage drops produced during ionization events
- Detector correction coefficients
- Implementation of the correction coefficients into the data analysis software

Optimal voltage determination would ensure the best stability and proper functioning of the modules. The evaluation of voltage drops would ensure that the detectors are never dropping to below their counting start voltage. And the correction coefficients would ensure reliable readings from all the detectors working simultaneously.

2.3. Optimal operating voltage determination

The determination of the optimal voltage involves determining the detectors plateau region. This is achieved by measuring the count rates at multiple voltages.

Four detector modules were selected using the "simple random sampling" method using the "lottery" technique. This method involves the random selection of subset samples out of a full set of samples. The samples were chosen based on the output of a random number generator (1-16). As each detector module had an equal probability of being selected, the selected modules should adequately represent the rest of the module's performance.

The methodology for determining the plateau region and optimal voltage range was as follows:

1. An initial supply voltage to the detectors was set to bellow the nominal operating voltage provided in the manufacturer's datasheet (Appendix 1). In this case the voltage was set to 280 Volts;
2. A source of ionizing radiation was placed near the module at a distance of 24 cm (the distance was selected arbitrarily);
3. Incrementing the voltage by 5 volts, with the module operating, a count start voltage was determined. The voltage at which the detector started registering any counts was noted as the count start voltage;
4. The source of ionizing radiation was removed;
5. The voltage was increased by 5 volts;
6. After a counting time of 1 minute the count rate was noted;
7. Steps 4 – 6 were repeated until the maximum voltage was reached;
8. The count rates at each voltage step were graphed as count rate dependency on supplied voltage;
9. By determining the region of the curve with lowest derivative we obtained an optimal operating voltage.

A note on step 7: ideally the maximum voltage would be determined by increasing the supply voltage to the internal gas breakdown voltage. This would give an accurate voltage at which the plateau region transitioned into the continuous discharge region. In this study, due to having limited amount of detectors, in order to preserve and not damage the GM tubes the voltage was increased up to a point where audible crackling was heard from inside the detector chamber, indicating that the voltage was very close to the breakdown voltage of the gas. The maximum voltage of the selected detectors was set to 410 Volts.

2.4. Voltage drop evaluation

The necessity for step 4 in the methodology described above (to remove the source) is due to the fact that when the detector registers an ionization event a voltage drop occurs. By noting down the set voltage with and without the source present these drops can be evaluated.

As with the determination of the optimal operating voltage the voltage drops were noted at each step of the voltage incrementation process, and then graphed. When selecting the operating voltage, it is critical to take into account the voltage drop caused by the presence of a source at the selected voltage value.

2.5. Determination of the detector correction coefficient

Every GM tube will have some variation in the readings it provides. This is largely dependent on the manufacturing of the GM tubes. Small variations in size, shape, and the mixture of inner gas may lead to identical detectors having different readings.

In order to determine the correction coefficients, the following methodology was used:

1. The detector modules were supplied with the optimal operating voltage;
2. The modules registered background activity for 10 minutes;
3. The total registered counts over 10 minutes were noted;
4. Steps 2 and 3 were repeated two more times resulting in a total of three measurements, 10 minutes each;
5. The results of the 3 measurements were averaged, resulting in the average number of counts per 10 minutes for each detector in the module;
6. The averages of the number of counts of each detector were then averaged;
7. The ratio of the overall number of counts ($COUNTS_{avr}$) and the average number of counts of the individual detector ($COUNTS_{avr,ij}$), where i is the module number and j is the detector number) gives the correction coefficient of the detector.

Equation (5) shows the determination of the correction coefficient (C_{corr}):

$$C_{corr} = \frac{COUNTS_{avr}}{COUNTS_{avr,ij}} \tag{5}$$

The correction coefficient serves a purpose of homogenizing the count rates of the detectors in order to provide consistent readings throughout the system.

2.6. Determination of detector deadtime

Determination of the detector deadtime was performed for 4 randomly selected modules. The procedure involved the use of two sources of ionizing radiation. The methodology used for this measurement was described in section 1.7.6. The following is a step-by-step overview of the methodology:

1. The count rate of the detector was measured using the first source at a distance of 24 cm over a period of 5 minutes;
2. The obtained count rate was noted;
3. Steps 1 and 2 were repeated two more times resulting in a total of 3 measurements;
4. Steps 1 – 3 were repeated for the same detector using a second source;
5. Steps 1 – 3 were repeated, this time using both sources simultaneously;
6. The obtained 3 sets of measurements were averaged;
7. Using the equation (4) from section 1.7.6 the deadtime of the detector was calculated.

The methodology described above was used for all 4 selected modules. A total of 8 deadtime values were determined for the 8 selected detectors. The obtained deadtime values were then averaged to represent the deadtime of the entire measurement system.

2.7. Determination of the dose rate conversion coefficient

To convert the count rate registered by the GM detectors it is necessary to apply a dose rate conversion coefficient. For the SBT-10 detector, the dose rate conversion coefficient was provided by the manufacturers technical datasheet. The provided coefficient was 322.5 CPS/µR/s, meaning that at a count rate of 322.5 counts per second is equivalent to 1 µR/s dose rate, assuming the source of ionizing radiation is cesium-137.

However, it is essential to note that this conversion coefficient might not remain constant over time due to potential aging effects of the detector. Therefore, it was deemed necessary to validate the coefficient to ensure its accuracy. The methodology to examine the conversion coefficient is outlined as follows:

1. Background dose rate was measured 10 times using a reliable handheld dosimeter (*DRG-01T1*);
2. The obtained values were averaged to obtain an average background dose rate value;
3. Background count rate measurements were performed for a total of 30 minutes (3 measurements, 10 minutes each) with the correction coefficients applied to all detectors;
4. Measurements from all detectors were averaged to obtain an average count rate over a period of 10 minutes.

The values obtained from this rigorous evaluation process were used to calculate the actual dose rate conversion coefficient. This determined value was then compared with the coefficient provided in the datasheet, allowing for a comparison, and ensuring the accuracy and reliability of the radiation detection system.

2.8. Experimental setup

The main setup for performing the measurements required for the determination of the optimal voltage and evaluation of the voltage drop can be seen in **Fig. 15**.

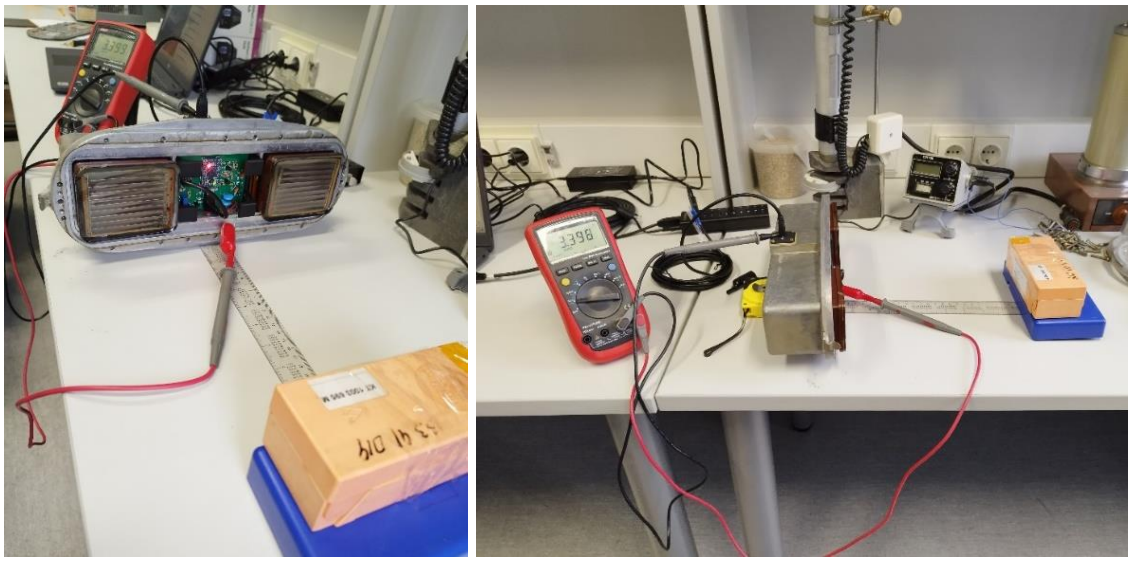

Fig. 15 Main measurement setup

The setup consisted of a GM module probed with a multimeter to display the current applied voltage to the module. The orange box containing a source of ionizing radiation was placed in-line with the detectors of the module at an arbitrary distance of 24 cm.

2.9. Software design specifications

The design of the software should be able to accommodate the modular design of the system. The main functionality of the software should be able to:

- Read and/or store the information provided by the Arduino microcontroller;
- Perform data accumulation;
- Apply the correction coefficients to the obtained data;
- Convert the obtained count rate into dose rate;
- Provide a user interface;
- Provide obtained data visualization;
- Retain reliable functionality, irrelevant of how many modules are connected to the system.

The programing language for the software was chosen to be the *python* programing language. *Python* offers an all-in-one solution for the incorporation of the required functionality and a GUI (graphical user interface). The design of the GUI was aided by an additional *python* GUI design tool *QtDesigner*, that uses the python *PyQt6* library for the creation of the GUI.

3. Results

3.1. Determination of the Geiger plateau region

Following the methodology described in section 2.3 the plateau the measurement data was collected and plotted to illustrate the plateau region. The measurement data can be found in **Table 3** (Appendix 2), and the plotted data can be seen in **Fig. 16**.

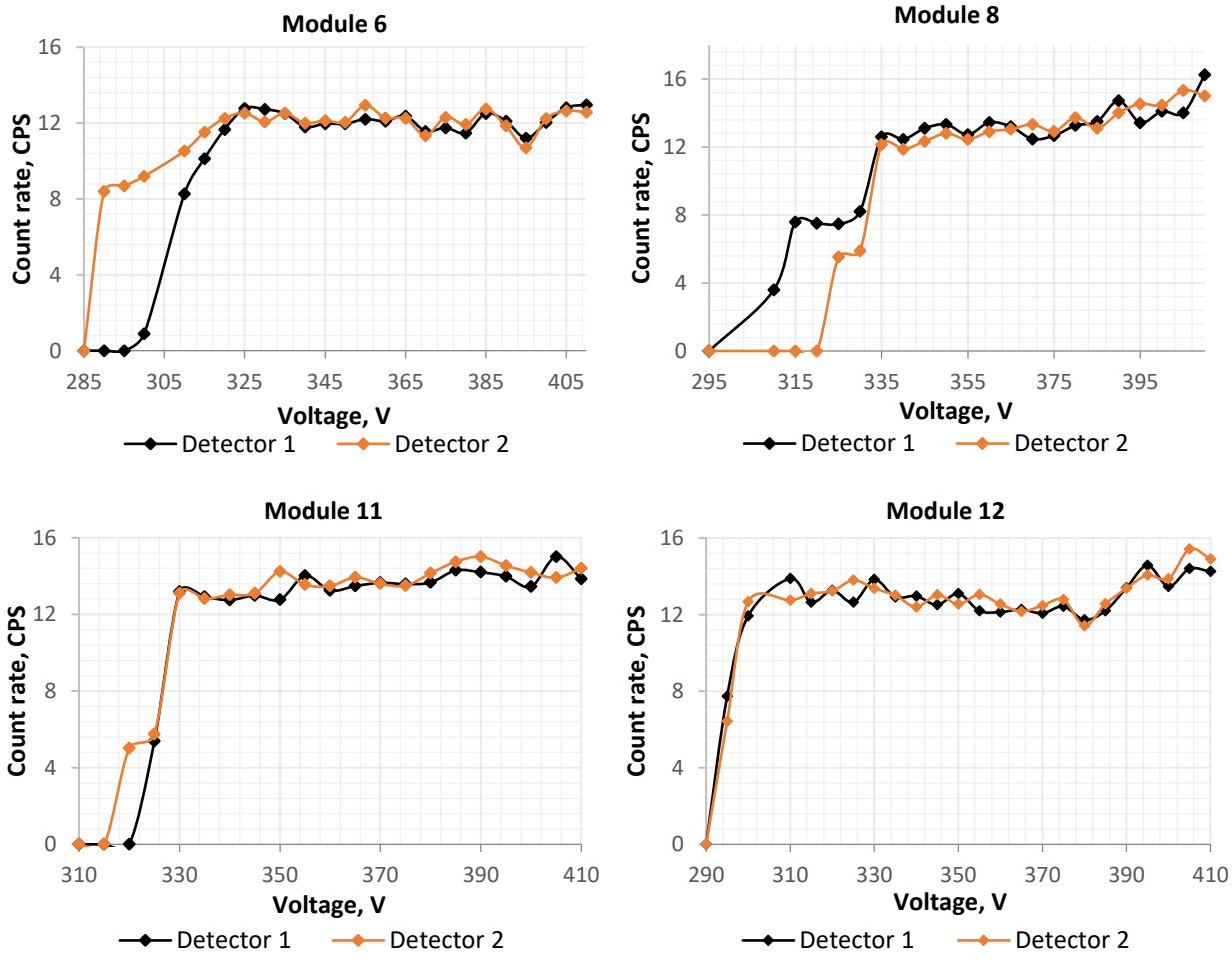

Fig. 16 Experimentally determined Geiger plateau region graphs

Based on the data we can determine the beginning and end of the plateau region. For module 6 the plateau regions for both detectors appear to start at a supplied voltage of 325 Volts. Module 8 had both detectors enter the plateau region at 335 Volts. Modules 11 and 12 have the beginning of the plateau region at 330 and 310 Volts respectively.

Due to reasons discussed in section 2.3 the end of the plateau region was set as 410 Volts. The true end of the plateau region may lay beyond the value of 410 Volts, since none of the detectors exhibited a continuous discharge at this voltage value.

To determine the optimal operating voltage, we can determine the most stable regions of the plateau curves. The optimal operating voltage should be chosen in this range. Module 6 exhibited the highest count stability in the region of 340 – 365 Volts, module 8 count rates remained stable in the range of 345 – 375 Volts. Module 11 and module 12 stable regions were determined to be 355 – 380 Volts, and 335 – 355 Volts respectively.

We can observe that not all modules have their most stable region in the same voltage ranges. Since not every single module in the system was tested, we must assume that the rest of the modules have their most stable count rates at similar voltage ranges. To find an operating voltage that could best be suitable for all the modules we can identify the overlapping range of stable voltage values. To find the overlapping range we can identify the highest lower limit and the lowest upper limit among the four ranges:

- Highest lower limit of the values 340, 345, 355, 335 is 355 Volts
- Lowest upper limit of the values 365, 375, 380, 355 is 355 Volts

In this case, the overlapping range is a single point at 355 Volts. Therefore, the single best voltage value for these modules would be 355 Volts.

3.2. Voltage drop evaluation

Each ionization event produces a voltage drop (ΔV) across the GM tube and as the count rate increases this voltage drop also tends to increase. The voltage drops across a range of detector operating voltages are plotted in the graphs shown in **Fig. 17**.

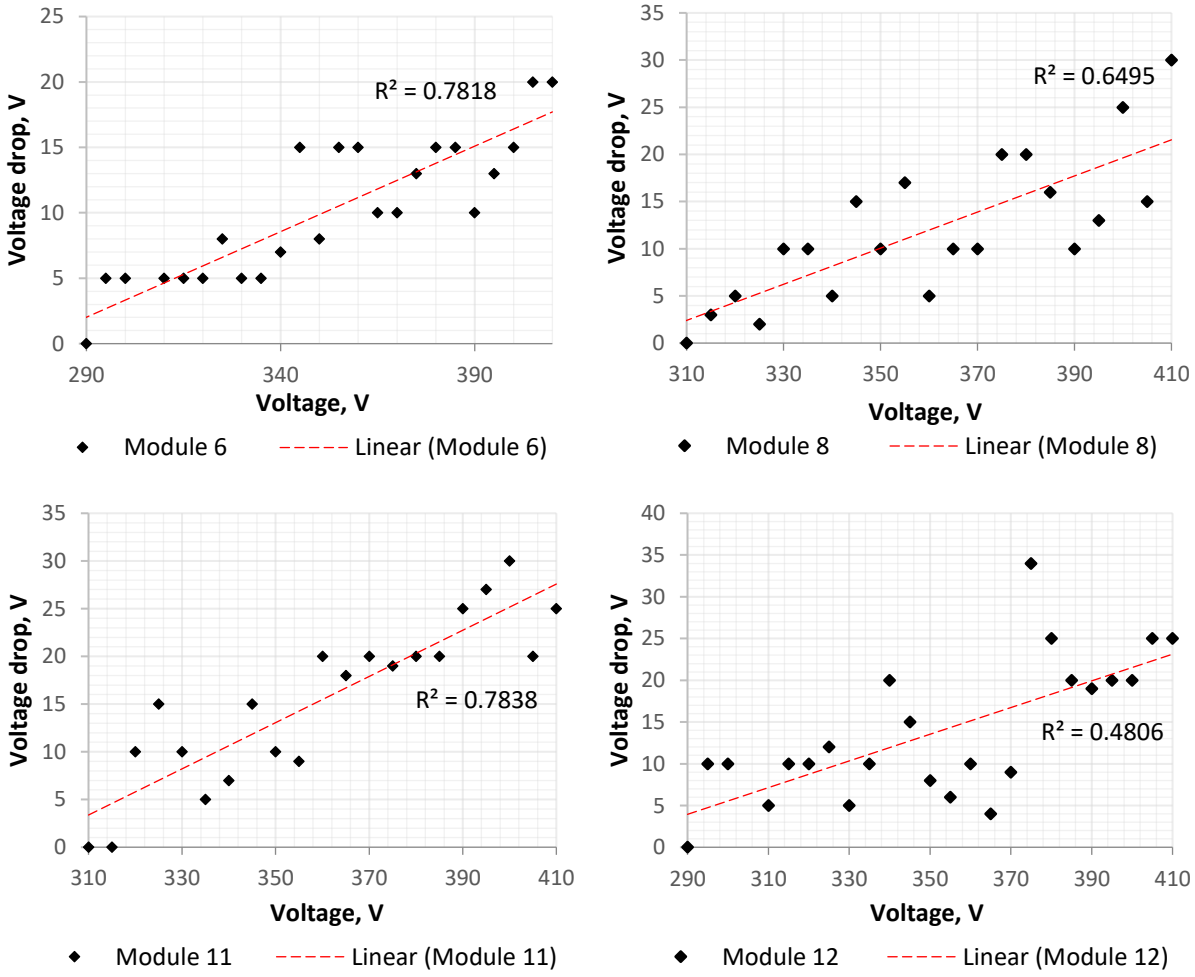

Fig. 17 Measured voltage drop across a range of supplied voltage graphs

As can be seen from the above graphs there appears to be no strong correlation between the applied voltage and the voltage drop, although in all four cases the voltage drop tends to increase as the applied voltage increases.

We can use the Pearson correlation coefficient (r), a common method to measure the linear correlation of the data:

$$r = \frac{\sum(x_i - \bar{x})(y_i - \bar{y})}{\sqrt{\sum(x_i - \bar{x})^2}\sqrt{\sum(y_i - \bar{y})^2}} \quad (6)$$

If: x_i – values of the x-variable in a sample; $\bar{x}$ – mean of the values of the x-variable; y_i – values of the y-variable in a sample; $\bar{y}$ – mean of the values of the y-variable.

The calculated Pearson coefficients for the investigated modules:

- Module 6: $r \approx 0.35$
- Module 8: $r \approx 0.45$
- Module 11: $r \approx 0.85$
- Module 12: $r \approx 0.75$

The Pearson coefficients indicate that that modules 11 and 12 show a moderate to strong linear trend as the values of the correlation coefficients are close to 1. This indicates that for these modules the relationship between ΔV and applied voltage may follow a linear pattern to some extent.

On the other hand, coefficients for module 6 and module 8 have weaker correlations. These coefficients indicate that there may be no strong linear dependency. Overall, the coefficients on their own are not enough to determine the linearity of the data as more in-depth statistical analysis is required.

Applying a higher voltage to the GM tubes the count rate increases slightly. This is due to the increased electric field in the tubes allowing for easier ionization of the gas, thus enhancing the detector efficiency, and in turn the count rate. These measurements of the voltage drop values can be used to assess the performance of the GM tubes at the selected operating voltage. In the case of the four tested modules the maximum voltage drop is not sufficient to drop the voltage to bellow the start of the plateau region.

3.3. Determination of detector correction coefficients

The GM modules' sensitivity can vary due to manufacturing differences or aging, making calibration necessary to ensure accurate measurements.

To assess the performance of each GM module, five measurements for each detector were made, where the software recorded the readings of the GM modules for one minute each. The results were noted to Table 1. The results showed the variation in the readings between the five measurements for each detector.

The correction coefficients were determined by taking the average of all module counts and dividing that average by each detector's average counts of the five measurements. This approach allowed to account for variations in the sensitivity of each detector and provide accurate correction coefficients. The results of the measurements are shown in **Table 1**.

Table 1 Detector measurement results and derived correction coefficients

Module No.	Detector No.	Measurement, counts			Average counts	Average CPS	Correction coefficient
		no. 1	no. 2	no. 3			
1	**1**	775	864	857	832	1.39	1.1316
	2	975	998	955	976	1.63	0.9646
2	**1**	832	818	775	808	1.35	1.1647
	2	778	799	817	798	1.33	1.1798
3	**1**	1102	1108	1137	1116	1.86	0.8439
	2	1207	1102	1190	1166	1.94	0.8072
4	**1**	850	808	856	838	1.40	1.1235
	2	834	844	943	874	1.46	1.0776
5	**1**	1052	1119	1058	1076	1.79	0.8747
	2	1004	1099	1078	1060	1.77	0.8879
6	**1**	1058	1069	566	898	1.50	1.0488
	2	919	944	962	942	1.57	0.9998
7	**1**	1128	1141	1058	1109	1.85	0.8490
	2	936	956	917	936	1.56	1.0055
8	**1**	984	1005	1040	1010	1.68	0.9325
	2	1017	977	1035	1010	1.68	0.9325
9	**1**	889	843	889	874	1.46	1.0776
	2	811	823	808	814	1.36	1.1566
10	**1**	767	811	849	809	1.35	1.1638
	2	877	948	850	892	1.49	1.0559
11	**1**	979	1024	1004	1002	1.67	0.9393
	2	901	964	967	944	1.57	0.9973
12	**1**	745	748	795	763	1.27	1.2345
	2	744	787	720	750	1.25	1.2548
13	**1**	1042	1021	1048	1037	1.73	0.9079
	2	985	1035	1029	1016	1.69	0.9264
14	**1**	744	858	781	794	1.32	1.1853
	2	748	756	717	740	1.23	1.2717
15	**1**	987	1037	1032	1019	1.70	0.9242
	2	986	957	971	971	1.62	0.9693
16	**1**	1208	1211	1152	1190	1.98	0.7909
	2	1020	1105	1064	1063	1.77	0.8857

The above table shows a variability in the measured counts for each detector in every module, with some detectors recording higher counts than others. This reinforces the need for deriving the calibration coefficients to ensure accurate measurements. The variations of the registered counts may be attributed to manufacturing differences, and aging effects.

The derived calibration coefficients for the detectors vary from 0.8053 to 1.2686. Values that are close to 1 indicate that the detector performs closely to the average performance of all detectors, with values above 1 showing performance of lower sensitivity, and values below 1 indicate a higher sensitivity of the detector.

By analyzing the average count or average count rate data we can assess relative errors between the individual detectors as well as relative errors between modules. Analyzing the relative errors within a module we can observe the smallest relative error of 0 % and the largest error of 15.57 %. The largest relative error between the performance of the modules was found to be 33.7 % with one of the modules (module 12) registering 756 counts on average and module 11 registering an average number of 1141 counts. These two modules appear to be the two largest outliers and require the largest and the smallest calibration coefficients to be applied.

Ideally the relative errors between the detectors and the modules should be as low as possible to ensure the most accurate measurements throughout the system. The detectors with largest relative errors were left in the system due to a lack of additional detectors on-hand. Adjusting the voltages of these modules to correct the sensitivity was not an option. This would have placed one module too close to the continuous discharge region and the other module too close to the starting voltage, risking either one of the modules to be damaged or the other failing to register any counts at all.

3.4. Determination of detector deadtime

Three sets of measurements were performed for the 4 selected modules. The obtained data was averaged and the deadtime for the detectors was calculated using these averaged values. The results of the measurements can be seen in **Table 2**. Source 1 and 2 columns show the averaged count rates under the exposure of the indicated source of ionizing radiation. The column marked as "combined" shows the average count rates of the detectors under the exposure of both sources simultaneously.

Table 2 Detector measurement results and derived deadtime values

Module No.	**Detector No.**	**Average count rate, CPS**			**Deadtime, µs**	**Average deadtime, µs**
		Source 1	**Source 2**	**Combined**		
3	**1**	112.116	94.396	200.480	284.938	870.413
	2	112.413	94.297	185.804	986.092	
13	**1**	109.700	100.710	193.940	745.721	
	2	102.380	95.600	182.320	799.877	
15	**1**	90.440	71.800	151.220	848.116	
	2	104.090	78.640	153.550	1782.364	
16	**1**	111.510	102.580	191.440	990.059	
	2	99.840	89.570	180.000	526.140	

The calculated deadtimes of the detectors were determined to be in the range of 248.938 – 1782.364 µs. Averaging these values, we calculate the average deadtime to be 0.870 µs.

Evaluation of the upper limit of the detectors count rates shows the variations of the largest count rates that can be reliably measured using these detectors. The range of the largest reliable count rates

was determined to be 561 – 4017 counts per second. Averaging this range, we get an average maximum count rate of 1148 counts per second.

The results of this deadtime determination show quite large variability in the performance of the selected detectors. Such differences in the deadtime measurements may indicate a degradation in quality of the detectors due to aging effects. Manufacturing differences may also contribute to these results.

Deadtime is only relevant when measuring high count rates, therefore, these detectors can still provide reliable readings at lower count rates. Since not all of the deadtime values for all detectors of the system were determined there is a possibility that other detectors might have even higher deadtimes, though from the obtained results we see that only a single detector exceeded a deadtime of 1 millisecond, it is reasonable to assume that such high deadtime values are not common in the system.

3.5. Determination of the dose rate conversion coefficient

According to the SBT-10 datasheet, provided by the manufacturer, the cesium calibrated sensitivity (Cs-137) is 322.5 CPS/μR/s. The conversion coefficient for converting R (roentgen) to Sv (sieverts) is 0.00933, so 1 μR/s becomes 0.00933 μSv/s. The formula for converting the count rate to dose rate in this case can be written like [53]:

$$D = CPS * CF \tag{7}$$

If: D – dose rate; CPS – counts per second; CF – conversion coefficient.

The provided sensitivity can be recalculated to obtain the conversion coefficient (CF) in the following manner:

$$\frac{322.5\ CPS}{1\ \mu\text{R/s}} = \frac{322.5\ CPS}{0.00933\ \mu\text{Sv/s}}$$

Converting μSv/s to μSv/h the equation becomes:

$$\frac{322.5\ CPS}{0.00933 * 3600\ \mu\text{Sv/h}} = \frac{322.5\ CPS}{33.588\ \mu\text{Sv/h}}$$

This gives a new value of the sensitivity in terms of CPS/μSv/h:

$$\frac{322.5\ CPS}{33.588\ \mu\text{Sv/h}} = 9.6016\ \text{CPS/}\mu\text{Sv/h}$$

The conversion coefficient can be the found by taking the inverse of the sensitivity, since we want to obtain a value for 1 CPS. The conversion coefficient was then calculated to be 0.1041 μSv/h/CPS. This means that a count rate of 1 CPS is equal to 0.1041 μSv/h.

Employing the methodology described in section 2.7, the average background dose rate was determined to be 0.134 μSv/h. The averaged count rate of the detectors with the applied correction coefficients was calculated to be 941 counts per 10 minutes. Converting this value to counts per second, a value of 1.569 CPS was obtained. Assuming, that a count rate of 1.569 CPS is equivalent

the measured background of 0.134 µSv/h, it was possible to calculate the dose rate for 1 CPS. The dose rate conversion coefficient was experimentally determined to be 0.0854 µSv/h/CPS.

By examining the obtained coefficients, we can see that there is a discrepancy between the conversion coefficient derived from the manufacturer's datasheet and the experimentally determined conversion coefficient. The former was calculated to be 0.1041 µSv/h/CPS, while the latter was determined to be 0.0854 µSv/h/CPS. The difference might be due to various factors such as experimental error or the inherent variability of the detector sensitivity. Furthermore, the manufacturer's coefficient could have been based on optimal or average conditions, which may not precisely mirror the specific conditions under which the experimental tests were performed. Therefore, this underlines the importance of carrying out in-situ calibrations and verifications to ensure accurate measurements.

By applying this conversion coefficient to the measured count rate, it is possible to estimate the dose rate. Precise dose rate cannot be determined using this method as GM counters by default assume that each count has the energy value of the gamma photon that it was calibrated with, in the case of the SBT-10 GM tube the assumption is that each count is registered from a cesium-137 source.

3.6. Software development

A custom software was designed for this measurement system. A screengrab of the GUI of the designed app (application) can be seen in **Fig. 18**.

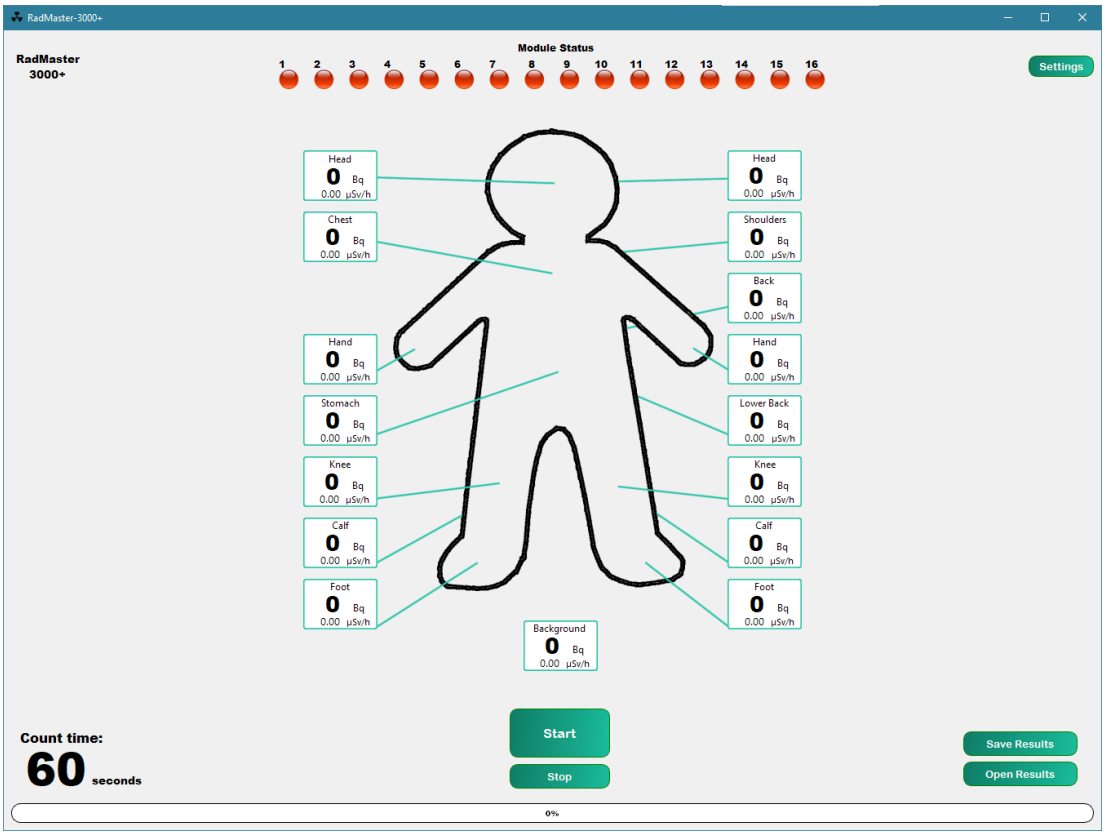

Fig. 18 Screengrab of the developed software

The GUI elements of the software include a real time display of the module readings, detection and indicators of the currently connected modules, a countdown timer, a progress bar, and the interaction buttons for various functions.

The software written for the readout and processing of the data consisted of multiple python files (.py) that call each other when necessary. The number of lines of code used in each python file was:

- Main.py – 223 lines
- Threads.py - 425 lines
- Ports.py - 88 lines
- GMapp.py - 230 lines
- RTout.py - 104 lines
- Var.py - 39 lines
- Layout.py - 2778 lines

This totals 3887 lines of code necessary for the functionality of this software. For the layout of the GUI (graphical user interface) *QtDesigner* software was used, meaning that the code for the layout was auto-generated. Not accounting for the layout.py file, the amount of hand-written code drops to 1109 lines.

A quick breakdown of the individual software file purposes:

- Main.py – the main application file which initializes the app window and manages GUI interactions;
- Threads.py – is the thread manager file. Various functions of the app (for example the real-time output) are initialized in their own threads for simultaneous functionality;
- Ports.py – this file contains the function to scan the serial ports of the computer and assigns individual COM ports to the modules;
- GMapp.py – the data acquisition file. In here the data transmitted by the modules is being read, and accumulated in the app's memory. The correction and conversion coefficients are applied to the raw data in this file;
- RTout.py – an auxiliary file to store the initial values of the variables required for the output of real-time data;
- Var.py – auxiliary file to store the various variables required for the functionality of the app;
- Layout.py – the GUI design file. This file contains only the GUI design code.

The basic workflow of the app is illustrated in the block diagram in **Fig. 19**.

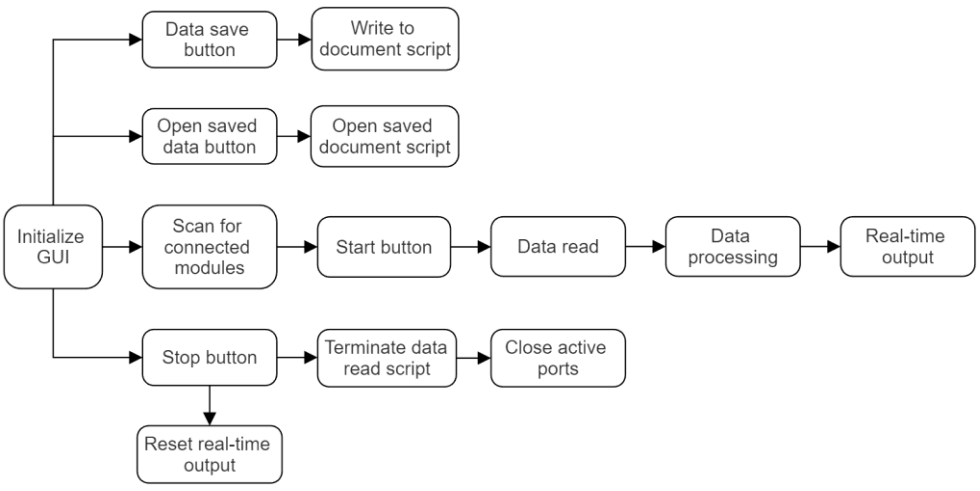

Fig. 19 Block diagram of the basic workflow of the software

The arrows in the diagram represent the initialization of the elements of the software. Upon launch the app initializes the main GUI. The GUI initialization consists of drawing the visual output of the software such as the data save/load buttons, and the start and stop buttons. Upon initialization the software scans all available serial ports and tries to identify the connected modules. If a module is found connected to the device the indicator turns from red to green. After the scan has been performed the measurements can start.

The start button initializes the main data read/data processing script that stores the incoming data as variables into the RTout.py file for real-time data display. The stop button is used to abort the measurement process and terminate the data read/process script, close all active serial ports, and reset the real-time display to zero. The data save/open buttons perform the simple tasks of writing the stored data to a document, and opening said document.

The software provides the necessary functionality for this radiometric system to be operable but may come with a few bugs in its current iteration as it was not designed by a software engineer. For optimal operation and stability, the software would require a redesign of the code structure. The open-source code of the software, along with the *Arduino* code can be found in Appendix 4 as a GitHub link to the project.

3.7. Final assembly

The assembly of the system required the dismantling the RZB-04-04 frame and stripping all of the original electronics and wiring. The original electronics were substituted for the custom designed boards (described in section 2.2).

The assembly also required the use of 3 USB hubs (10 USB ports each), and 3 external power supply blocks for power delivery to the USB hubs. The power supplies were necessary due to the system requiring long connection cables due to the construction of the support frame of the detector modules. In practice, any cable inherently provides some voltage loss due to internal resistance of the cable, and long cables, in particular may drop the voltage sufficiently that the main circuit boards would be supplied with insufficient voltage required for operation.

In addition to each module being operated by an *Arduino* microcontroller, the dosimetry frames' original start button was also equipped with an *Arduino* for communication with the main software.

220 Volt mains power was supplied to the system which was then stepped down to 5 Volts by the 3 AC/DC converters (alternating current to direct current). Each individual USB hub was supplied with 5 Volts by their respective converters. The supplied power was then transmitted via USB cables to the external start button and the modules. The operating principle of the modules was described in section 2.2.

Data transmission was established by USB cables. Each module was connected via cable to a USB hub. Modules 1, 3, 5, 7, 9, and 11 were connected to USB hub 1. Modules 2, 4, 6, 8, 10, 12 were connected to USB hub 2. The rest of the modules (13, 14, 15, and 16) were connected to USB hub 3. The data registered by the modules was then transmitted to the computer equipped with the analysis software through the USB hubs. The external start button, used for the initialization of measurement, communicated with the software through USB hub 1. A block diagram of the system can be seen in **Fig. 20**. The block diagram shows the elements of the system along with the established connections,

where the red lines represent the power lines of the system and the blue lines represent the data transmission lines.

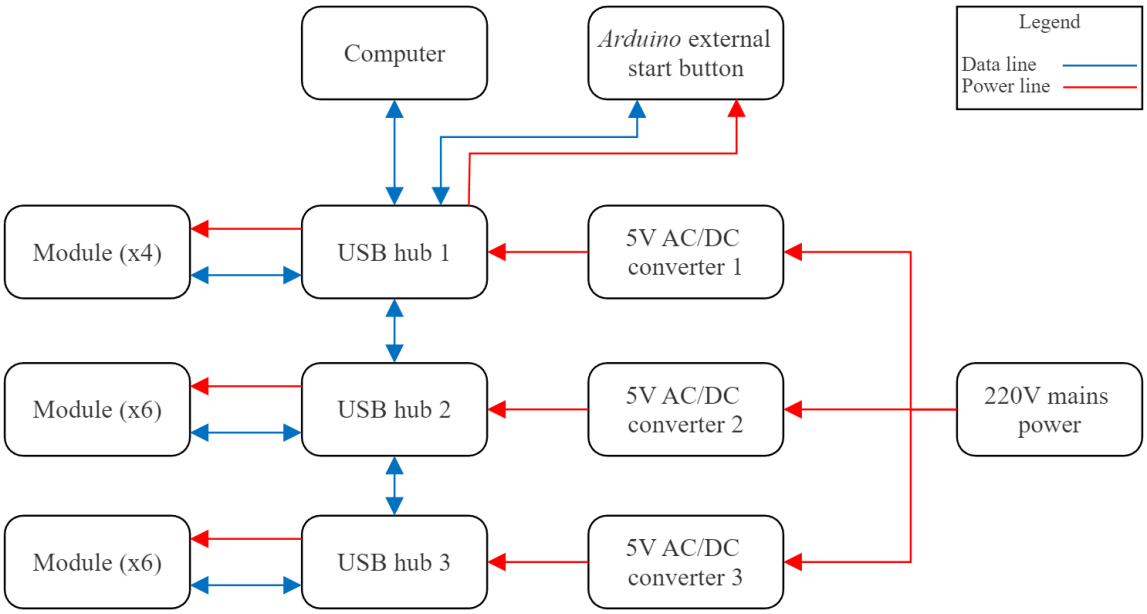

Fig. 20 Block diagram of the developed modular radiometric measurement system

The user interface of the system consisted of a *Lenovo ThinkCentre TIO22Gen3* touchscreen monitor equipped with a *Lenovo ThinkCentre M715q Tiny* computer shown in **Fig. 21**.

Fig. 21 *ThinkCentre TIO22Gen3* monitor (left) and *ThinkCentre M715q* computer (right)

The monitor used to interface with the system was an all-in-one model, meaning it was designed with a special housing to host the computer within itself. This type of design not only preserves the theme of a modular design but also eliminates the need for additional dedicated space to host the computer. The specifications of the computer are listed below:

- *Ryzen 5 Pro 2600GE* processor (CPU),
- 8 gigabytes of random-access memory (RAM)
- 160 gigabytes of SSD (solid-state drive) storage

The computers powerful CPU and the good amount of memory (both random-access and storage) ensure the smooth performance of the software.

Most of the original electronics of the system were installed in a special cavity inside the frame. The cavity contained two GM tube detectors (background reference), a high voltage transformer, and unidentified circuit. The original electronics can be seen in **Fig. 22**.

Fig. 22 Component cavitity with original electronics

For this project the cavity was equipped with an *ICY BOX IB-AC6110* 10-port USB hub, and the 5 Volt AC/DC converter (**Fig. 23**). The cavity also fitted the background reference detectors. The detectors were installed on the cover plate of the cavity.

Fig. 23 *ICY BOX* USB hub (left), 5 Volt AC/DC converter (middle), component cavity (right)

The remaining two *ICY BOX* USB hubs and AC/DC converters were installed in other, smaller component cavities in order to not overcrowd the main cavity and provide better cable management.

The fully assembled and functioning modular radiometric measurement system can be seen in **Fig. 24**

Fig. 24 Assembled modular radiometric measurement system (1 – left frame, 2 – middle frame, 3 – left and middle cavity, 4 – right cavity, 5 – bottom cavity, 6 – bottom module housing, 7 – monitor arm)

Thirteen detector modules were housed in the left (**Fig. 24-1**) and middle (**Fig. 24-2**) frame of the system. The left frame housed 6 modules while the middle frame hosted 7 modules. Two ICY BOX USB hubs and two 5 Volt AC/DC converters were installed into the cavities (**Fig. 24-3**) of the left and middle frame (1 hub and 1 converter each). The third USB hub along with its voltage converter was installed into the right frames (**Fig. 24-4**) cavity. The cavity's cover plate was equipped with background reference detectors (facing into the cavity). The bottom cavity (**Fig. 24-5**) of the right frame acted as a power distribution hub. Mains power would be inserted into the power input and from there distributed to the three 5 Volt AC/DC converters. The remaining two detector modules were installed into the bottom housing (**Fig. 24-6**). This housing also contained an Arduino microcontroller, and a momentary switch that engaged when the middle frame would be pulled back. This momentary switch was connected to the Arduino and upon engaging sent out a signal to the software to initiate a measurement. Finally, to hold the interface components of the system, a monitor arm (**Fig. 24-7**) was used.

Conclusions

1. The overview of the modular radiometric systems has provided insights into the benefits of such an approach to radiometry, including scalability, cost-effectiveness, ease of maintenance, and flexibility. Modular systems can offer a wide range of applications ranging from area monitors and personnel dosimetry to both static and mobile environmental monitoring. Current modular radiometric measurement system solutions show promise in the field of radiation protection and dosimetry. With advancements in technology, modular systems may benefit from innovations and evolve further, providing more flexibility and scalability.
2. A single radiometry module was designed and assembled. The module consisted of two square-chamber Geiger-Mueller tubes, and a main circuit board. The main circuit board functionality was two-fold: to generate a high voltage current required for the functionality of the GM tubes, and condition the signal obtained from the GM tubes. The board was also was equipped with an *Arduino* microcontroller that served as a data interpreter and as a link to the designed software.
3. Multiples of the designed radiometry module were produced, totaling 16 independent modules. The modules, and by extension, the GM tubes within the modules exhibited variations in sensitivity of detection, therefore, calibration coefficients were derived for each detector. The calibration coefficients ranged from 0.8053 to 1.2686 indicating relatively good group operation quality. With these coefficients implemented into the software the count rate of the modules showed to be more uniform. The optimal voltage was derived from analyzing the detectors Geiger-Mueller (plateau) region and was determined to be 355 Volts. Voltage drop evaluation was performed using a source of ionizing radiation and was determined to be irrelevant for the count rate of the detectors. Finally, a dose rate conversion coefficient of 0.0854 was experimentally determined for the SBT-10 detectors.
4. Dedicated software was developed in *python* programming language for interacting with the modules and for data analysis. The software is capable of real-time count rate and dose rate display, automated start and stop of the measurement system, and data export functionality. While the current software iteration may have some limitations, it serves as a foundation for further improvement and optimization. The developed system offers a versatile and customizable solution for radioactivity detection and dosimetry.

List of references

1. BEQUEREL, A H. On the invisible rays emitted by phosphorescent bodies. *Comptes Rendus*. November 1896. Vol. 122, no. 1358, pp. 420–421 ISSN 00280836.
2. CURIE, Marie. On the heat dissipated by a platinum surface at high temperatures. *Proceedings of the Royal Society of London* [online]. 31 December 1898. Vol. 63, no. 389, pp. 403–405 ISSN 0370-1662. Available from: doi: 10.1098/rspl.1898.0050.
3. BULLETIN OF THE ATOMIC SCIENTISTS. World's Most Dangerous Toy? Radioactive Atomic Energy Lab Kit with Uranium (1950). *Bulletin of the Atomic Scientists* [online]. [viewed 1 May 2023]. Available from: https://thebulletin.org/virtual-tour/worlds-most-dangerous-toy-radioactive-atomic-energy-lab-kit-with-uranium-1950/
4. UNITED NATIONS. SCIENTIFIC COMMITTEE ON THE EFFECTS OF ATOMIC RADIATION. *Sources and effects of ionizing radiation: UNSCEAR 1993 report to the General Assembly* [online]. United Nations, 1993. [viewed 23 April 2023]. ISBN 9211422000. Available from: //www.unscear.org/unscear/en/publications/1993.html
5. LINDELL, Bo, DUNSTER, John and VALENTIN, Jack. International Commission on Radiological Protection. *The British Journal of Radiology* [online]. 1971. Vol. 44, no. 526, pp. 2–3 ISSN 0007-1285. Available from: doi: 10.1259/0007-1285-44-526-814.
6. UNITED NATIONS SCIENTIFIC COMMITTEE ON THE EFFECTS OF ATOMIC RADIATION (UNSCEAR). Sources and Effects of Ionizing Radiation, United Nations Scientific Committee on the Effects of Atomic Radiation UNSCEAR 2000 Report to the General Assembly, with Scientific Annexes. *UNSCEAR 2000 Report*. 2000. Vol. I, pp. 6–9 ISSN 0144-8420, 1742-3406.
7. INTERNATIONAL ATOMIC ENERGY AGENCY (IAEA). Radiation Protection and Safety of Radiation Sources: International Basic Safety Standards. *Radiation Protection and Safety of Radiation Sources: International Basic Safety Standards* [online]. 2014. p. 5 [viewed 23 April 2023]. Available from: https://www.iaea.org/publications/8930/radiation-protection-and-safety-of-radiation-sources-international-basic-safety-standards
8. FRY, R. J. M. and HALL, Eric J. Radiobiology for the Radiologist. *Radiation Research* [online]. March 1995. Vol. 141, no. 3 ISSN 00337587. Available from: doi: 10.2307/3579017.
9. PAWLICKI, Todd, et al. Hendee's Radiation Therapy Physics. In : *Hendee's Radiation Therapy Physics* [online]. 2016. p. 5–9. ISBN 978-0-470-37651-5.
10. BRENNER, David J. and HALL, Eric J. Computed Tomography — An Increasing Source of Radiation Exposure. *New England Journal of Medicine* [online]. 29 November 2007. Vol. 357, no. 22, pp. 16–26 ISSN 0028-4793. Available from: doi: 10.1056/nejmra072149.
11. ALSHAREF, Shomokh, et al. Review about radiopharmaceuticals: Preparation, radioactivity, and applications. *International Journal of Applied Pharmaceutics* [online]. 2020. Vol. 12, no. 3, pp. 8–15 ISSN 09757058. Available from: doi: 10.22159/IJAP.2020V12I3.37150.
12. HENDEE, William R. and MARC EDWARDS, F. ALARA and an integrated approach to radiation protection. *Seminars in Nuclear Medicine* [online]. 1 April 1986. Vol. 16, no. 2, pp. 142–150 ISSN 00012998. Available from: doi: 10.1016/S0001-2998(86)80027-7.
13. DO, Kyung Hyun. General Principles of Radiation Protection in Fields of Diagnostic Medical Exposure. *Journal of Korean Medical Science* [online]. 2016. Vol. 31, no. 1 ISSN 15986357. Available from: doi: 10.3346/JKMS.2016.31.S1.S6.

14. GOLDSTONE, Karen E. Principles and control methods. MARTIN, Colin J. and SUTTON, David G. (eds.), *Practical Radiation Protection in Health Care*. 2015. Vol. 1, pp. 82–93
15. FUJIWARA, Kenji, et al. Fulminant hepatitis and late onset hepatic failure in Japan. *Hepatology Research* [online]. 2008. Vol. 38, no. 7, pp. 646–657 ISSN 13866346. Available from: doi: 10.1111/j.1872-034X.2008.00322.x.
16. YUSOF, N. and HILMY, N. Radiation Biology of Tissue Radiosterilization. *Comprehensive Biomedical Physics* [online]. 1 January 2014. Vol. 7, pp. 263–287 Available from: doi: 10.1016/B978-0-444-53632-7.00813-3.
17. ICRP. Annals of the ICRP Published on behalf of the International Commission on Radiological Protection International Commission on Radiological Protection Main Commission of the ICRP Corresponding members. *Annals of the ICRP* [online]. 2009. No. 109, pp. 15–17 Available from: doi: 10.1177/ANIB_37_2-4.
18. O'CONNOR, U., et al. Recommendations for the use of active personal dosemeters (APDs) in interventional workplaces in hospitals. *Physica Medica* [online]. 1 July 2021. Vol. 87, pp. 131–135 ISSN 1120-1797. Available from: doi: 10.1016/J.EJMP.2021.05.015.
19. KRANER, H.W. Radiation detection and measurement. *Proceedings of the IEEE* [online]. 1981. Vol. 69, no. 4 ISSN 0018-9219. Available from: doi: 10.1109/PROC.1981.12016.
20. KNEŽEVIĆ, Željka, et al. Investigations into the basic properties of different passive dosimetry systems used in environmental radiation monitoring in the aftermath of a nuclear or radiological event. *Radiation Measurements* [online]. 1 August 2021. Vol. 146 ISSN 13504487. Available from: doi: 10.1016/j.radmeas.2021.106615.
21. KRON, Tomas, LEHMANN, Joerg and GREER, Peter B. Dosimetry of ionising radiation in modern radiation oncology. *Physics in medicine and biology* [online]. 28 June 2016. Vol. 61, no. 14, pp. 167–205 ISSN 1361-6560. Available from: doi: 10.1088/0031-9155/61/14/R167.
22. MCKEEVER, S.W.S., MOSCOVITCH, M. and TOWNSEND, P.D. Thermoluminescence dosimetry materials: properties and uses. . 1995. p. 159–164
23. CLAIRAND, I., et al. Use of active personal dosemeters in interventional radiology and cardiology: Tests in laboratory conditions and recommendations - ORAMED project. *Radiation Measurements* [online]. 1 November 2011. Vol. 46, no. 11 ISSN 13504487. Available from: doi: 10.1016/j.radmeas.2011.07.008.
24. AHMED, Syed Naeem. Physics and engineering of radiation detection. *Choice Reviews Online* [online]. 2007. Vol. 45, no. 02, pp. 45–48 ISSN 0009-4978. Available from: doi: 10.5860/choice.45-0892.
25. FERNANDEZ, Bernard. From the discovery of the atomic nucleus to the DWBA, a (short) history of nuclear reactions, and of the instruments which permitted their study. .
26. POPIC, Jelena Mrdakovic, et al. Assessment of radionuclide and metal contamination in a thorium rich area in Norway. *Journal of Environmental Monitoring* [online]. June 2011. Vol. 13, no. 6, pp. 23 ISSN 14640325. Available from: doi: 10.1039/C1EM10107B.
27. MCMASTER UNIVERSITY. Chapter 3 Gas Filled Detectors 3.1. Ionization chamber A. Ionization process and charge collection. *Radioisotopes and Radiation Methodology* [online]. [viewed 27 December 2021]. Available from: https://www.science.mcmaster.ca/radgrad/images/6R06CourseResources/4RA34RB3_Lecture_Note_3_GasFilled-Detectors.pdf

28. KRŽANOVIĆ, Nikola, et al. Harmonization of IEC type testing requirements and test methods for active area dosimeters in environmental monitoring. *Radiation Physics and Chemistry* [online]. 1 September 2022. Vol. 198 ISSN 18790895. Available from: doi: 10.1016/j.radphyschem.2022.110291.
29. FUJIBUCHI, Toshioh, TOYODA, Takatoshi and TERASAKI, Kento. Measurement of basic characteristics of scintillation-type radiation survey meters with multi-pixel photon counter. *Applied Radiation and Isotopes* [online]. 1 October 2018. Vol. 140, pp. 12–17 ISSN 18729800. Available from: doi: 10.1016/j.apradiso.2018.06.010.
30. BAEZA, A., et al. Calibration of an air monitor prototype for a radiation surveillance network based on gamma spectrometry. *Applied Radiation and Isotopes* [online]. 1 May 2014. Vol. 87, pp. 57–60 ISSN 0969-8043. Available from: doi: 10.1016/J.APRADISO.2013.11.095.
31. KRŽANOVIĆ, Nikola, et al. Development and testing of a low cost radiation protection instrument based on an energy compensated Geiger-Müller tube. *Radiation Physics and Chemistry* [online]. 1 November 2019. Vol. 164 ISSN 0969-806X. Available from: doi: 10.1016/J.RADPHYSCHEM.2019.108358.
32. SAULI, Fabio. Gaseous radiation detectors: Fundamentals and applications. *Gaseous Radiation Detectors: Fundamentals and Applications* [online]. 1 January 2011. p. 6–8 Available from: doi: 10.1017/CBO9781107337701.
33. LEO, William R. *Techniques for Nuclear and Particle Physics Experiments* [online]. Springer Berlin Heidelberg, 1994.
34. KILLEEN, P. G., MWENIFUMBO, C. J. and FORD, K. L. Tools and Techniques: Radiometric Methods. *Treatise on Geophysics: Second Edition* [online]. 1 January 2015. Vol. 11, pp. 447–524 Available from: doi: 10.1016/B978-0-444-53802-4.00209-8.
35. PETER SIEGEL. Introduction to Geiger Counter. *California State Polytechnic University* [online]. [viewed 27 December 2021]. Available from: https://www.cpp.edu/~pbsiegel/phy432/labman/geiger.pdf
36. ALBERT S KESTON. Geiger-muller counter. *Google Patents* [online]. 27 October 1944. [viewed 27 December 2021]. Available from: https://patents.google.com/patent/US2409498
37. OLLEGOTT, Kevin, et al. Fundamental Properties and Applications of Dielectric Barrier Discharges in Plasma-Catalytic Processes at Atmospheric Pressure. *Chemie Ingenieur Technik* [online]. 10 October 2020. Vol. 92, no. 10 ISSN 0009-286X. Available from: doi: 10.1002/cite.202000075.
38. ANALOG.COM. CN0536 Circuit Note | Analog Devices. *Analog.com* [online]. 2015. [viewed 27 December 2021]. Available from: https://www.analog.com/en/design-center/reference-designs/circuits-from-the-lab/cn0536.html#rd-description
39. MASSACHUSETTS INSTITUTE OF TECHNOLOGY. Geiger-Müller counter circuit theory. *MIT OpenCourseWare* [online]. [viewed 27 December 2021]. Available from: https://ocw.mit.edu/courses/nuclear-engineering/22-s902-do-it-yourself-diy-geiger-counters-january-iap-2015/readings/MIT22_S902IAP15_geigr_ckt.pdf
40. UNITED STATES REGULATORY COMMISSION. What Is A Geiger Counter? | NRC.gov. *U.S. NRC* [online]. 19 May 2020. [viewed 27 December 2021]. Available from: https://www.nrc.gov/reading-rm/basic-ref/students/science-101/what-is-a-geiger-counter.html
41. KRANE, Kenneth S. *Handbook of Particle Detection and Imaging* [online]. Cham : Springer International Publishing, 2020. ISBN 978-3-319-47999-6.

42. BELL, Daniel and WONG, Monica. Ionisation chamber. In : *Radiopaedia.org* [online]. Radiopaedia.org, 2019.
43. SPAAN, Bernhard and STEVENS, Holger. Particle Physics: In : *Elementary Particle Physics in a Nutshell* [online]. Princeton University Press, 2011. p. 1–8. ISBN 9783110785968.
44. L'ANNUNZIATA, Michael F. *Handbook of Radioactivity Analysis* [online]. Elsevier Inc., 2013. ISBN 9780123848734.
45. VOSE, PETER B. Detection Systems and Instrumentation. *Introduction to Nuclear Techniques in Agronomy and Plant Biology* [online]. 1980. p. 46–76 Available from: doi: 10.1016/B978-0-08-024924-7.50011-9.
46. NUCLEAR POWER. Townsend Avalanche. *nuclear-power.com* [online]. [viewed 2 May 2023]. Available from: https://www.nuclear-power.com/nuclear-engineering/radiation-detection/gaseous-ionization-detector/operating-regions-of-ionizing-detectors-detector-voltage/townsend-avalanche/
47. KNOLL, Glenn F. Radiation detection and measurement. . 2010. p. 830
48. CENTRONICS LTD. Geiger Muller tubes, a guide to applications and characteristics. [online]. [viewed 21 December 2022]. Available from: https://web.archive.org/web/20150919220104/http://www.centronic.co.uk/downloads/Geiger_Tube_theory.pdf
49. ALMUTAIRI, Bader, et al. Experimental evaluation of the deadtime phenomenon for GM detector: deadtime dependence on operating voltages. *Scientific Reports 2020 10:1* [online]. 17 November 2020. Vol. 10, no. 1, pp. 1–15 [viewed 27 May 2022]. ISSN 2045-2322. Available from: doi: 10.1038/s41598-020-75310-3.
50. RYDE, S. J. S. Practical gamma-ray spectrometry. *Rapid Communications in Mass Spectrometry* [online]. 1 January 1995. Vol. 9, no. 12, pp. 73–75 ISSN 0951-4198. Available from: doi: 10.1002/rcm.1290091227.
51. HIRAM COLLEGE. *Geiger-Müller Counter and Nuclear Counting Statistics PART I Geiger Tube: Optimal Operating Voltage and Resolving Time*. [no date].
52. EMARIETE.COM. How does a Geiger counter work? Its 6 characteristics. *eMariete.com* [online]. 2022. [viewed 21 December 2022]. Available from: https://emariete.com/en/how-does-a-geiger-muller-counter-works/
53. HOLOVATYY, Andriy, et al. Development of Microcontroller-Based System for Background Radiation Monitoring. *Sensors 2020, Vol. 20, Page 7322* [online]. 20 December 2020. Vol. 20, no. 24 ISSN 1424-8220. Available from: doi: 10.3390/S20247322.
54. IVASHEVA, A.Yu., BORISOV, V.S. and SEMENIKHIN, P.V. Adjusting of the detection efficiency of Geiger-Muller counters in the energy range of gamma radiation from 50 to 3000 keV. *Journal of Physics: Conference Series* [online]. December 2018. ISSN 1742-6588. Available from: doi: 10.1088/1742-6596/1135/1/012042.
55. RUSSELL-PAVIER, Frederick S., et al. A highly scalable and autonomous spectroscopic radiation mapping system with resilient IoT detector units for dosimetry, safety and security. *Journal of Radiological Protection* [online]. 1 March 2023. Vol. 43, no. 1 ISSN 0952-4746. Available from: doi: 10.1088/1361-6498/acab0b.
56. VARELA, João. Electronics and data acquisition in radiation detectors for medical imaging. *Nuclear Instruments and Methods in Physics Research Section A: Accelerators, Spectrometers,*

Detectors and Associated Equipment [online]. 11 July 2004. Vol. 527, no. 1–2, pp. 21–26 ISSN 0168-9002. Available from: doi: 10.1016/J.NIMA.2004.03.011.

57. ALDENER, Mattias, et al. SAUNA III - The next generation noble gas system for verification of nuclear explosions. *Journal of Environmental Radioactivity* [online]. 1 June 2023. Vol. 262, pp. 107–159 ISSN 18791700. Available from: doi: 10.1016/j.jenvrad.2023.107159.
58. SCOTT TELOFSKI, J., et al. RadNet Radiological Air Monitoring Network. *Controle (Paris)*. 2010. p. 134–142 ISSN 1254-8146.
59. RSC (RADIATION SECURITY CENTER). RADIS monitoring system. *EURDEP* [online]. 2021. [viewed 12 May 2023]. Available from: https://www.rsc.lt/index.php/pageid/1196
60. MCCLARREN, Ryan G. Curve Fitting. In : *Computational Nuclear Engineering and Radiological Science Using Python*. 2018. p. 193–214. ISBN 9780128122532.
61. AGOSTINELLI, S., ALLISON, J. and AMAKO, K., et al. Geant4—a simulation toolkit. *Nuclear Instruments and Methods in Physics Research Section A: Accelerators, Spectrometers, Detectors and Associated Equipment* [online]. 1 July 2003. Vol. 506, no. 3, pp. 250–303 ISSN 0168-9002. Available from: doi: 10.1016/S0168-9002(03)01368-8.
62. BADAMASI, Yusuf Abdullahi. The working principle of an Arduino. *Proceedings of the 11th International Conference on Electronics, Computer and Computation, ICECCO 2014* [online]. 23 December 2014. Available from: doi: 10.1109/ICECCO.2014.6997578.
63. LUFF, R., et al. Open-source hardware and software and web application for gamma dose rate network operation. *Radiation Protection Dosimetry* [online]. 1 August 2014. Vol. 160, no. 4, pp. 252–258 ISSN 0144-8420. Available from: doi: 10.1093/RPD/NCU012.
64. MONDADA, Francesco, et al. Bringing Robotics to Formal Education: The Thymio Open-Source Hardware Robot. *IEEE Robotics and Automation Magazine* [online]. 1 March 2017. Vol. 24, no. 1, pp. 77–85 ISSN 10709932. Available from: doi: 10.1109/MRA.2016.2636372.
65. IMAGES SI INC. DIY Geiger Counter. [online]. [viewed 3 May 2023]. Available from: https://www.imagesco.com/articles/geiger/build_your_own_geiger_counter.html
66. MARCU, Ioana, et al. Overview of IoT basic platforms for precision agriculture. *Lecture Notes of the Institute for Computer Sciences, Social-Informatics and Telecommunications Engineering, LNICST* [online]. 2019. Vol. 283, pp. 124–137 ISSN 18678211. Available from: doi: 10.1007/978-3-030-23976-3_13/COVER.
67. BARÓ, J., et al. PENELOPE: An algorithm for Monte Carlo simulation of the penetration and energy loss of electrons and positrons in matter. *Nuclear Instruments and Methods in Physics Research Section B: Beam Interactions with Materials and Atoms* [online]. 1 May 1995. Vol. 100, no. 1, pp. 31–46 ISSN 0168-583X. Available from: doi: 10.1016/0168-583X(95)00349-5.
68. XU, X. George. An exponential growth of computational phantom research in radiation protection, imaging, and radiotherapy: a review of the fifty-year history. *Physics in Medicine & Biology* [online]. 21 August 2014. Vol. 59, no. 18 ISSN 0031-9155. Available from: doi: 10.1088/0031-9155/59/18/R233.
69. Health Physics Instrumentation. In : *Radiation Protection and Dosimetry* [online]. New York, NY : Springer New York, 2003. p. 132–177.
70. KHAMTUIKRUA, Chaowanan and SUKSOMPONG, Sirilak. Awareness about radiation hazards and knowledge about radiation protection among healthcare personnel: A quaternary care academic center–based study. *SAGE Open Medicine* [online]. 2020. Vol. 8 ISSN 20503121. Available from: doi: 10.1177/2050312120901733.

71. BONACCORSI, Andrea and ROSSI, Cristina. Why open source software can succeed. *Research Policy* [online]. 1 July 2003. Vol. 32, no. 7, pp. 1243–1258 ISSN 00487333. Available from: doi: 10.1016/S0048-7333(03)00051-9.
72. VON HIPPEL, Eric. Democratizing innovation: The evolving phenomenon of user innovation. *Journal fur Betriebswirtschaft* [online]. March 2005. Vol. 55, no. 1, pp. 63–78 ISSN 03449327. Available from: doi: 10.1007/s11301-004-0002-8.
73. LAZER, David M.J., et al. The science of fake news: Addressing fake news requires a multidisciplinary effort. *Science* [online]. 9 March 2018. Vol. 359, pp. 1094–1096 ISSN 10959203. Available from: doi: 10.1126/science.aao2998.
74. NASCIMENTO, Susana and PÓLVORA, Alexandre. Opening up technologies to the social: Between interdisciplinarity and citizen participation. *Design Issues* [online]. October 2013. Vol. 29, no. 4, pp. 31–40 ISSN 07479360. Available from: doi: 10.1162/DESI_a_00228.

Appendices

Appendix 1. SBT-10(A) and SBT-11(A) technical datasheet

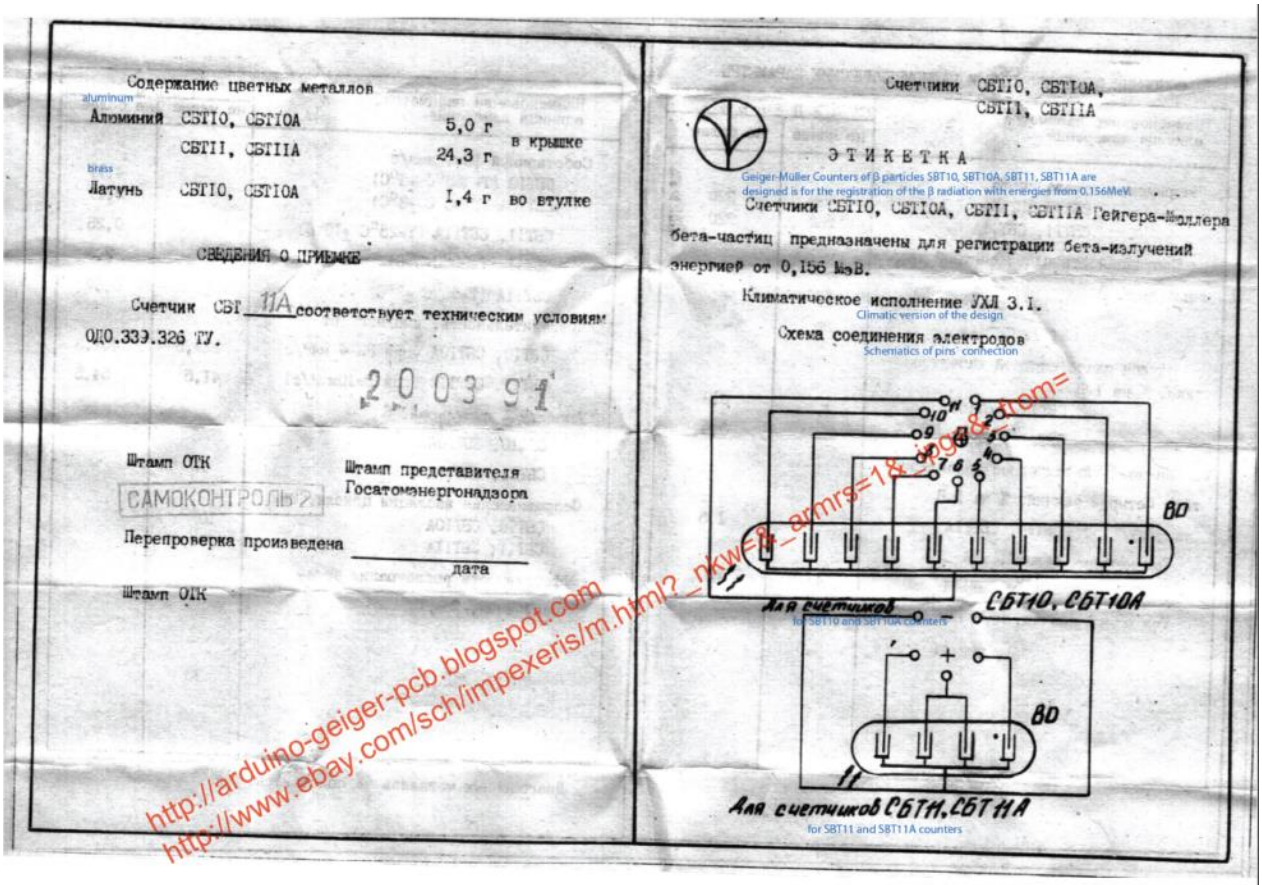

Содержание цветных металлов

aluminum

Алюминий СБТ10, СБТ10А 5,0 г в крышке
СБТ11, СБТ11А 24,3 г

brass

Латунь СБТ10, СБТ10А 1,4 г во втулке

СВЕДЕНИЯ О ПРИЕМКЕ

Счетчик СБТ 11А соответствует техническим условиям ОДО.339.326 ТУ.

20391

Штамп ОТК

САМОКОНТРОЛЬ

Штамп представителя Госатомэнергонадзора

Перепроверка произведена _____ дата

Штамп ОТК

Счетчики СБТ10, СБТ10А, СБТ11, СБТ11А

ЭТИКЕТКА

Geiger-Müller Counters of β particles SBT10, SBT10A, SBT11, SBT11A are designed is for the registration of the β radiation with energies from 0.156MeV.

Счетчики СБТ10, СБТ10А, СБТ11, СБТ11А Гейгера-Мюллера бета-частиц предназначены для регистрации бета-излучений энергией от 0,156 МэВ.

Климатическое исполнение УХЛ 3.1.

Climatic version of the design

Схема соединения электродов

Schematics of pins' connection

Для счетчиков СБТ11, СБТ11А

for SBT11 and SBT11A counters

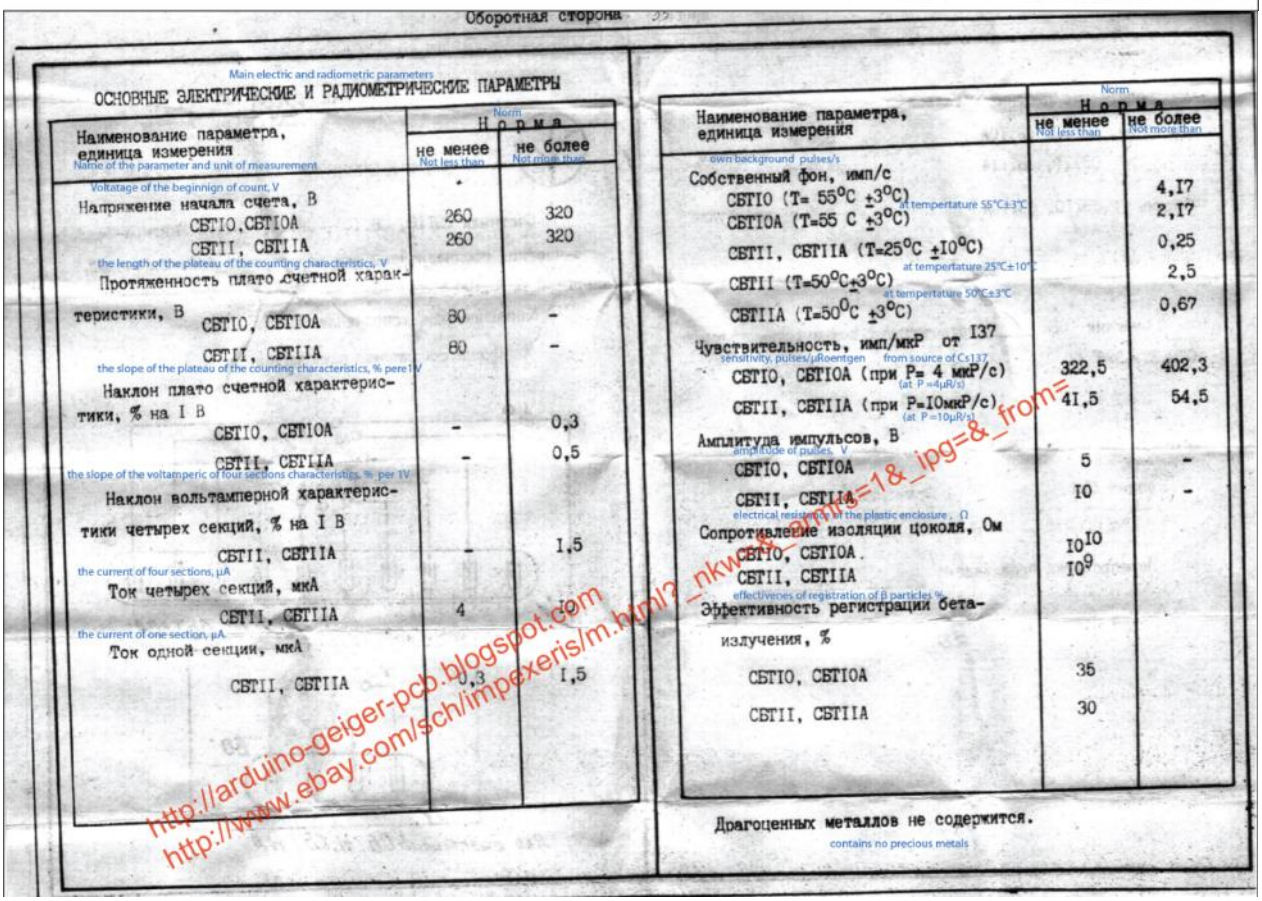

Оборотная сторона

Main electric and radiometric parameters

ОСНОВНЫЕ ЭЛЕКТРИЧЕСКИЕ И РАДИОМЕТРИЧЕСКИЕ ПАРАМЕТРЫ

Наименование параметра, единица измерения Name of the parameter and unit of measurement	Норма Norm не менее Not less than	Норма Norm не более Not more than
Напряжение начала счета, В Voltage of the beginnign of count, V		
СБТ10, СБТ10А	260	320
СБТ11, СБТ11А	260	320
Протяженность плато счетной характеристики, В the length of the plateau of the counting characteristics, V		
СБТ10, СБТ10А	80	-
СБТ11, СБТ11А	80	-
Наклон плато счетной характеристики, % на 1 В the slope of the plateau of the counting characteristics, % per 1V		
СБТ10, СБТ10А	-	0,3
СБТ11, СБТ11А	-	0,5
Наклон вольтамперной характеристики четырех секций, % на 1 В the slope of the voltamperic of four sections characteristics, % per 1V		
СБТ11, СБТ11А	-	1,5
Ток четырех секций, мкА the current of four sections, μA		
СБТ11, СБТ11А	4	10
Ток одной секции, мкА the current of one section, μA		
СБТ11, СБТ11А	0,3	1,5

Наименование параметра, единица измерения	Норма Norm не менее Not less than	Норма Norm не более Not more than
Собственный фон, имп/с own background pulses/s		
СБТ10 (Т= 55°С ±3°С) at tempertature 55°C±3°C		4,17
СБТ10А (Т=55 С ±3°С)		2,17
СБТ11, СБТ11А (Т=25°С ±10°С) at tempertature 25°C±10°C		0,25
СБТ11 (Т=50°С±3°С) at tempertature 50°C±3°C		2,5
СБТ11А (Т=50°С ±3°С)		0,67
Чувствительность, имп/мкР от Cs137 sensitivity, pulses/μRoentgen from source of Cs137		
СБТ10, СБТ10А (при Р= 4 мкР/с) (at P =4μR/s)	322,5	402,3
СБТ11, СБТ11А (при Р=10мкР/с) (at P =10μR/s)	41,5	54,5
Амплитуда импульсов, В amplitude of pulses, V		
СБТ10, СБТ10А	5	-
СБТ11, СБТ11А	10	-
Сопротивление изоляции цоколя, Ом electrical resistance of the plastic enclosure, Ω		
СБТ10, СБТ10А	10^{10}	
СБТ11, СБТ11А	10^{9}	
Эффективность регистрации бета-излучения, % effectiveness of registration of β particles %		
СБТ10, СБТ10А	35	
СБТ11, СБТ11А	30	

Драгоценных металлов не содержится.

contains no precious metals

Appendix 2. Measurement results of the determination of the Geiger plateau region (table)

Table 3 Geiger plateau region determination measurement data

Voltage	Count rate, CPS							
	Module 6		Module 8		Module 11		Module 12	
	Det. 1	Det. 2	Det. 1	Det. 2	Det. 1	Det. 2	Det. 1	Det. 2
285	0	0	0	0	0	0	0	0
290	0	8.4	0	0	0	0	0	0
295	0	8.7	0	0	0	0	7.73	6.43
300	0.9	9.2	0	0	0	0	11.93	12.67
310	8.27	10.53	0	3.6	0.00	0.00	13.88	12.75
315	10.13	11.53	0	7.6	0.00	0.00	12.64	13.1
320	11.67	12.25	0	7.51	0.00	5.02	13.27	13.23
325	12.77	12.53	5.53	7.47	5.38	5.75	12.64	13.8
330	12.73	12.07	5.9	8.21	13.18	13.10	13.83	13.37
335	12.5	12.52	12.14	12.6	12.92	12.82	12.92	13.01
340	11.8	12	11.87	12.45	12.75	13.02	12.97	12.4
345	11.97	12.13	12.34	13.1	12.98	13.10	12.51	13.03
350	11.96	12.05	12.8	13.33	12.77	14.23	13.1	12.55
355	12.21	12.94	12.45	12.73	14.02	13.55	12.2	13.05
360	12.1	12.27	12.91	13.45	13.25	13.48	12.13	12.54
365	12.38	12.25	13.05	13.2	13.48	13.93	12.27	12.17
370	11.57	11.34	13.33	12.47	13.65	13.60	12.07	12.47
375	11.75	12.31	12.93	12.67	13.58	13.50	12.43	12.78
380	11.48	11.93	13.73	13.27	13.67	14.15	11.73	11.41
385	12.51	12.75	13.1	13.5	14.30	14.75	12.2	12.56
390	12.1	11.86	14.02	14.73	14.20	15.02	13.4	13.37
395	11.2	10.7	14.54	13.43	13.98	14.55	14.57	14.07
400	12.03	12.23	14.46	14.1	13.45	14.18	13.47	13.87
405	12.81	12.64	15.34	14.01	15.02	13.92	14.4	15.43
410	12.97	12.57	15.02	16.26	13.85	14.40	14.25	14.9

Appendix 3. Main circuitry schematics used for in the modules

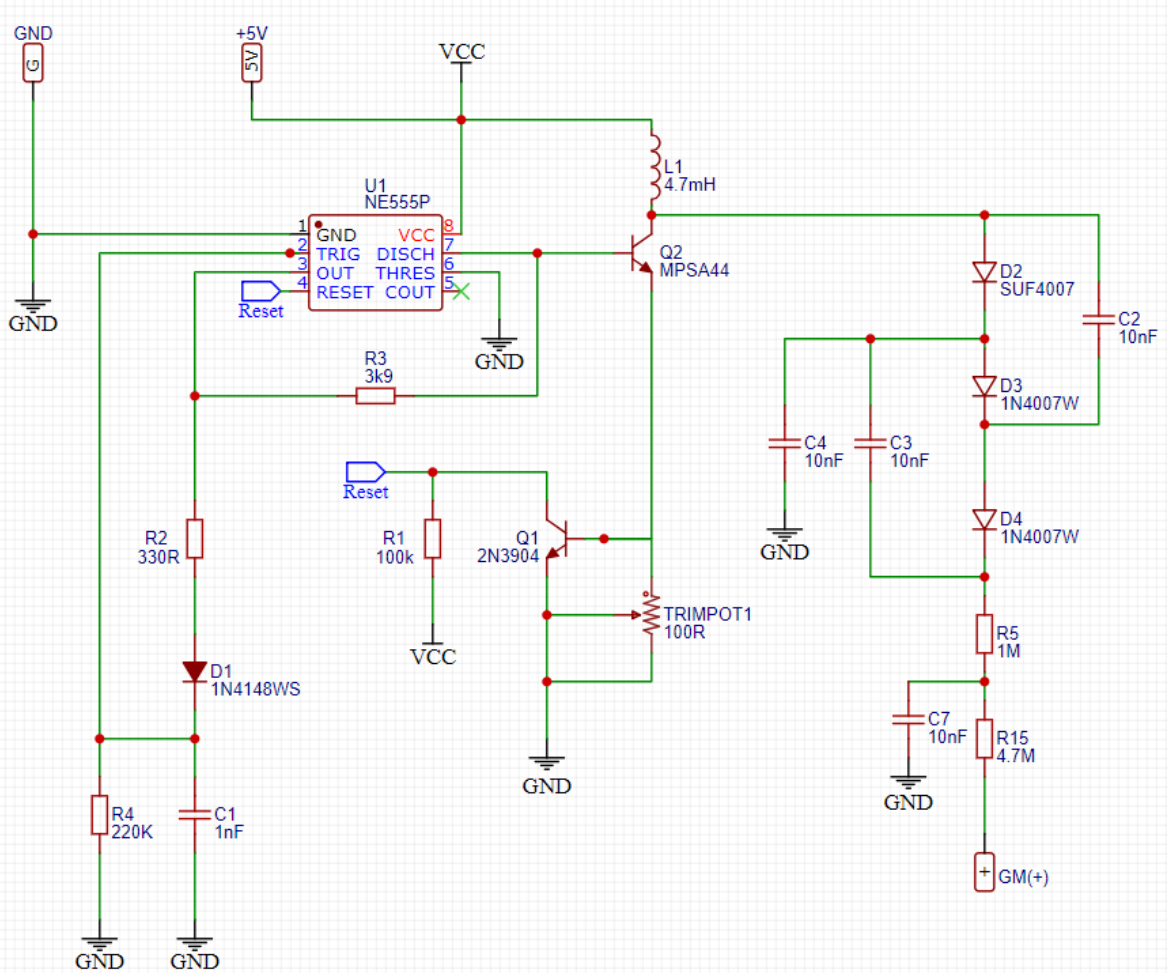

Fig. 25 HV generator circuit diagram

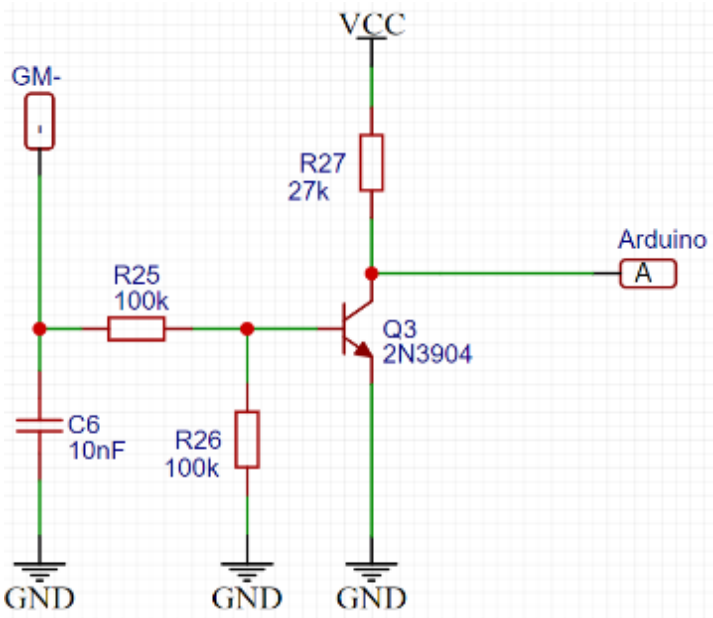

Fig. 26 Arduino signal conditioning circuit diagram

Appendix 4. *GitHub* project repository link

The repository contains the *Arduino* source code used by the modules as well as the source code of the *python* software.

Link: https://github.com/AndriusDievas/RadMaster-3000